AN ABSTRACT OF THE THESIS OF

Walter Eugen Frick for the degree Master of Science

in Atmospheric Sciences presented 18 Feb. 1976.

Title: THE INFLUENCE OF STRATIFICATION ON PLUME STRUCTURE.

Abstract approved: Redacted for Privacy

Larry J. Mahrt

In plume theory it is generally assumed that a plume issuing from a round source maintains a round cross section throughout. The consequences of this hypothesis are significant; this fact should motivate research into its validity. This paper investigates conditions and analyzes mechanisms that cause fluid plumes to undergo systematic deformation in their cross section. The process of deformation is referred to as differential growth. In search of support for these ideas some available plume experiments are investigated and some supporting evidence is found and presented. It is argued that ambient wind and variations in vertical buoyancy cause these effects. A rudimentary examination of plume physics tends to support these ideas. Approximations for these mechanisms are developed. For simplicity an important approximation is made in characterizing the plume cross section with an ellipse. By way of illustrating the effect of such cross sections on plume dynamics the computer plume model of Winiarski and Frick is adapted for differential growth. Based on the results of these modifications of the model compared with round plume results and compared with some plume data it is found that the modified model is able to predict behavior the conventional theory does not predict.

The Influence of Stratification on Plume Structure

by

Walter Eugen Frick

A THESIS

submitted to

Oregon State University

in partial fulfillment of
the requirements for the
degree of

Master of Science

Completed 6 June 1975

Commencement June 1977

APPROVED:

Redacted for Privacy

Assistant Professor of Atmospheric Sciences in charge of major

Redacted for Privacy

Chairman of Department of Atmospheric Sciences

Redacted for Privacy

Dean of Graduate School

Date thesis is presented: 6 June 1975

Typed by Walter Eugen Frick

TABLE OF CONTENTS

LIST OF ILLUSTRATIONS

THE INFLUENCE OF STRATIFICATION ON PLUME STRUCTURE

INTRODUCTION

The threat of environmental pollution caused by industrial plumes has largely sustained the effort to develop a reliable and general plume model. Through the years many models have been proposed; these have ranged from early rules of thumb to the fairly complex and complete models developed recently. Nevertheless, because of the difficulty of the problem there is still room for more work and for fresh ideas.

At the present stage of development numerous simplifying assumptions are made in any model. One of the most important simplifications involves the round plume hypothesis. This presumes that a plume issuing from a round orifice remains round in any cross section over its trajectory. It is proposed here that this hypothesis is generally inadequate; simultaneously too restrictive in describing the plume while dominant in determining the behavior of what remains. However, evidence which shows that the round plume hypothesis is inadequate is not abundant or obvious. Actually, any kind of experimental plume data are scarce; data which would decide this question forcefully and conclusively are non-existant. For these reasons the round plume hypothesis is not easily challenged. Plume experience is sufficient so that some people question the hypothesis but, to this point in time, not seriously enough to abandon it.

The round plume hypothesis is its own best reason for its existence in that it enormously simplifies the differential equations governing plume behavior. The processes that cause the plume, initially round, to take on some other shape are very complex. A complete plume

model usually includes five or more differential equations. Describing the processes leading to other cross sections would complicate the existing equations and add others. However the problem is not as dismal as it may seem and it is felt that a start should be made to understand and model these processes.

In this thesis it is proposed that an elliptical plume cross section represents plume realities better than the circular cross section. Generating mechanisms are found and approximated in numerical terms. An unconventional plume model developed by Winiarski and Frick (16) is adapted for these mechanisms. It is believed that careful study of this model and its modifications will be rewarded by a fuller understanding of the topic than is possible with more conventional, but physically more remote, plume models. At the outset it should be understood that this is not intended to be the last word written on the subject of plume cross sections or plume dynamics. The purpose of this paper is to attempt to develop the subject clearly enough and convincingly enough so that an impetus for further work will be created.

However tentative some of the approximations made in this thesis concerning the mechanisms governing the formation of non-circular cross sections, the fundamental plume principles of the basic model are not altered. What results is a picture of plume behavior that is perhaps not adequate in quantitative terms, however, the results of the theory bear a striking resemblance to some experimentally observed results that previous theories do not and can not predict.

II THE ROUND PLUME HYPOTHESIS

The round plume hypothesis is firmly entrenched in modern plume theory even as it is sometimes disparaged by plume theorists. The use of the round plume hypothesis relative to actual plume behavior would perhaps be adequate for any but the finer points were not the radius of the plume directly tied to the entrainment process. Entrainment is the process whereby ambient fluid is mixed into the body of the plume. An analytical expression for this process based on first principles has not been developed and in order to obtain closure of the plume equations an expression for it has to be formulated. Traditionally entrainment is related with proportionality constants to several characteristics of the plume, e.g. velocity shear, or the vertical velocity, and, most importantly, to the plume radius. Upon experimental verification of these "constants" they are shown to vary appreciably over a range of conditions. The attempt may then be made to resolve differences by conducting extensive experimental work in order to define observed variations. Alternatively other mechanisms may be introduced to account for apparent differences; for example, solid body drag concepts may be included. Whatever is done, the obvious bond of entrainment to the radius of a circle is very dominant in determining the magnitude of entrainment but is ignored as a source of error and a place to search for improvement.

To illustrate how the round plume hypothesis might lead to the difficulties mentioned consider the following. Suppose it is given that entrainment is proportional to the circumference of the plume. If it is assumed that the plume cross section is round then the circumference is

$2\pi r$, where r is the nominal radius of the plume. (It should be understood that this radius is usually measured vertically through the axis of the plume.) The entrainment is then $2\pi r C_1$ where C_1 is the coefficient of proportionality. Suppose next that the cross section is in fact elliptical, then entrainment is actually proportional to $2\pi[(f^2 + b^2)/2]^{1/2}$, where f and b are the ellipse's major and minor axes respectively. If the constant of proportionality is C_2, the success of the round plume hypothesis requires that,

$$1. \qquad 2\pi[(f^2 + b^2)/2]^{1/2} C_2 = 2\pi r C_1 .$$

Since it is given that C_2 is constant this can only be satisfied for variable r if C_1 is variable also. The attempt to describe the variations of C_1 with experimental work would be a poor substitute for the actual facts because the interaction between the radius and other variables may be ignored.

Before complicating existing models by using elliptical cross sections it is necessary to show that significant deviations from roundness occur. Abramovich (1) shows the elongated horseshoe shape that the cross section takes on just a few diameters from the source: results are shown in Figure 1. Scorer (12), in discussing bifurcation of plumes, qualitatively constructs his cross sections the same way. It has long been known that plumes rising into very stable air, i.e. fanning plumes, flatten significantly as they rise and reach their equilibrium elevation. In this case the effect appears generally to be ascribed to diffusion yet it can be noted that sometimes the plume reaches a maximum vertical width and subsequently narrows farther from the source. (A good example of this can be seen in the photographs in Ref. 17.) For

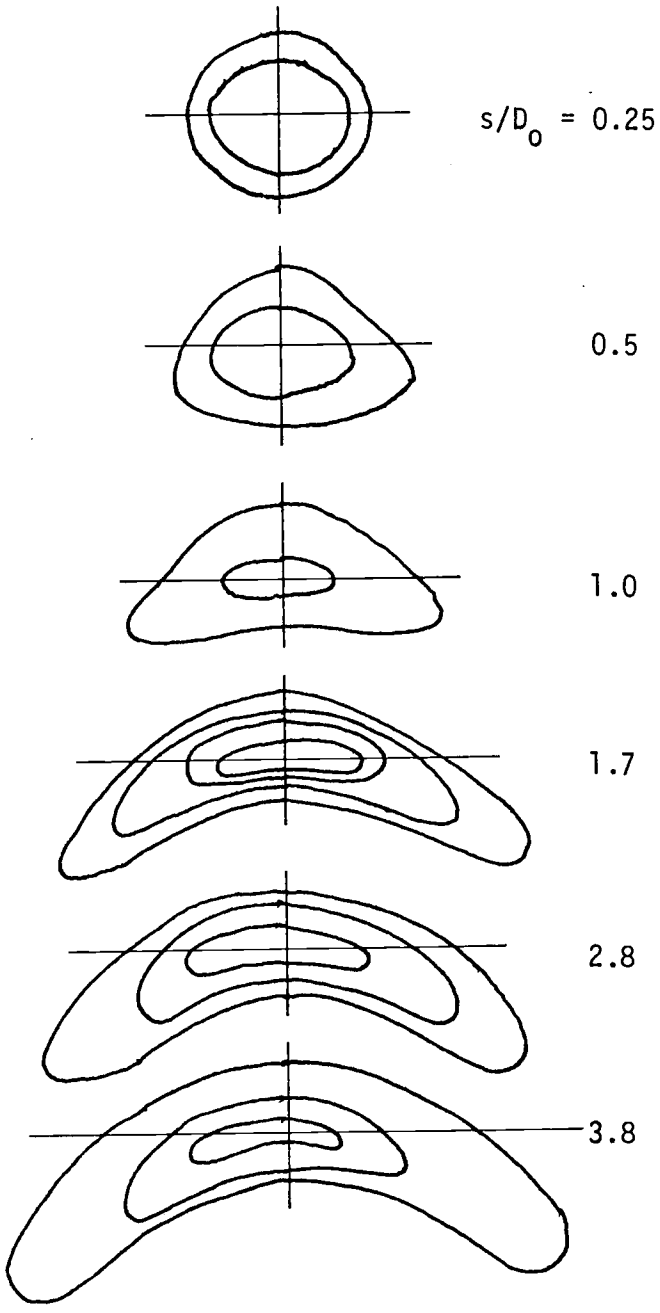

Figure 1. Plume cross sections at various distances from the source (expressed as the ratio of distance along the trajectory to the initial radius). After Abramovich (1).

this to be explained by diffusion arguments would require negative diffusion. Subsequently it will be explained how adiabatic cooling of the plume in a stratified environment can lead to the observed results.

Direct evidence of the alleged un-round nature of plumes and, by implication, of differential growth (the different rate of growth of the cross section in one coordinate direction compared with the other), is otherwise very limited. Ayoub (2) took pictures of plumes from side and top simultaneously in a laboratory setting. Unfortunately the buoyant plume was discharged horizontally into a flowing cross stream in water: he wanted to separate jet from buoyant effects. The geometry of the experimental setup precludes most differential growth from differential buoyancy. The lack of other simultaneous photography is an important deficiency because in simply looking at a plume, from a given point, acquiring perspective is almost impossible. In other words, the three dimensional nature of plumes is not apparent because the usual visual clues necessary for perspective are absent.

Some direct experimental evidence of the deformation of initially round plume cross sections can be obtained from the LIDAR work on chimney plumes conducted by P.M. Hamilton (7). LIDAR imagery can give almost instantaneous two dimensional profiles of the plume. The sample cross section available is far from round--being flattened considerably.

Fan (5) took the trouble of actually obtaining plume cross sections for Froude numbers 20 and 40. The results are presented in Figure 2. (Froude number is defined as:

$$2. \qquad Fr = v_o/[2r_o g(\rho_o - \rho_a)/\rho_a]^{1/2}.$$

Here ρ_o and ρ_a are the source and ambient densities respectively, v_o is

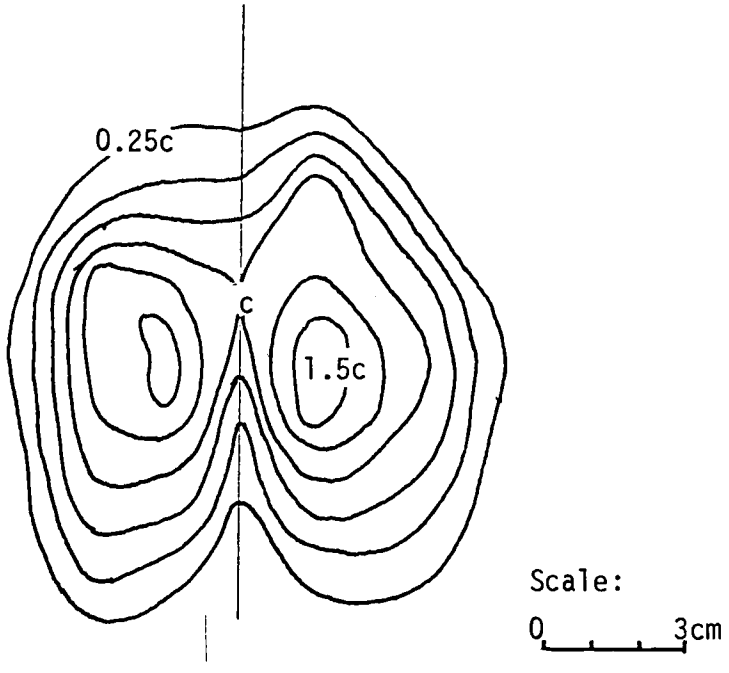

A. Fr. = 40, K = 8, s/D_o = 32.5, and c = 0.059. c represents maximum centerline concentration.

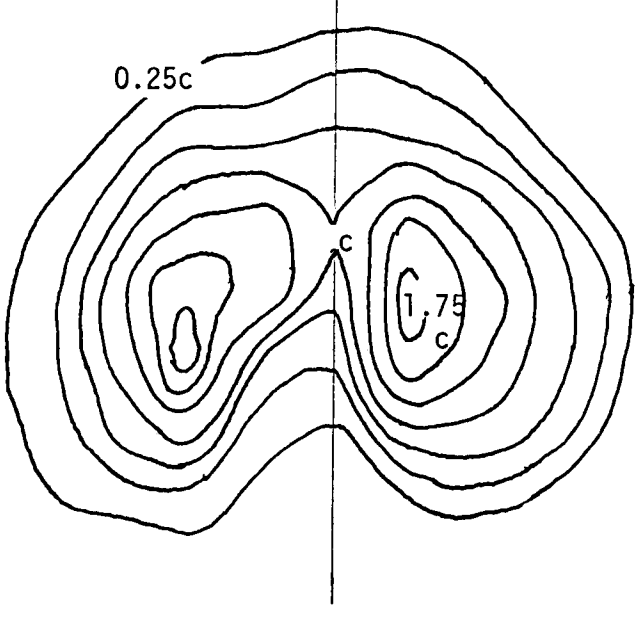

B. Fr. = 20, K = 8, s/D_o = 37.0, and c = 0.036. c represents maximum centerline concentration.

Figure 2. Experimentally observed plume cross sections, after Fan (5).

the source exit velocity and r_o is the source radius. The number is a relative measure of the ratio of momentum and buoyancy initially present; the smaller the Froude number is the more buoyancy dominates over momentum in determining plume characteristics. Other factors equal, the smaller the Froude number the greater the rise of the plume.) The case Fr = 20 is seen to be approximated well in a general way by an ellipse. It can be seen by examining Fan's photographs that the plumes are fairly steady and it is believed that these cross sections reproduce instantaneous characteristics very faithfully even though averaging times at a given point are about a minute long.

Work somewhat analogous to Fan's was conducted by Hewett, Fay and Hoult (8) on air plumes in a wind tunnel with a temperature stratification capability. They present a cross section for a case in unstratified ambient air; it is virtually round. The initial impression is that differential growth is insignificant or absent. Unfortunately a case corresponding to a stratified environment is not presented. Had that capability been used it may still have led to inconclusive results because under these circumstances internal circulations were set up in the tunnel which would have countered the transverse flattening of the plume. Also, the distance from the source is not specified so that it is not possible to ascertain how much uniform growth has occured since differential growth all but ceased as the plume leveled off. (If an object, initially elliptical, enlarges uniformly on all sides it will become proportionally more circular.) Moreover, the cross section can be mimicked by starting with dimensions proportional to Fan's case for Fr = 20, and effectively allowing it to oscillate vertically about half a diameter and

horizontally one quarter its diameter. Then graphically averaging the isopleths by superimposing four identical cross sections over each other the prescribed distances apart results in a composite cross section very similar to the one described. This exercise should be valid since the air plume cannot be as well controlled as a water plume and will not be as steady. It should also be valid because of the long averaging times used in obtaining the cross sections. Finally, the Froude number used makes it apparent that the initial excess plume temperature is on the order of $100^{o}C$ which places the Boussinesq approximations into question. This will not necessarily invalidate anything but what complications may result are not clear.

Indirect evidence of differential growth can be found by studying Figure 3 which presents data correlation curves based on Fan's experimental data (13). The data come from about 90 sets of measurements made on water plumes. The plumes were negatively buoyant salt plumes and were discharged downward into a flowing cross stream. The Froude number range was 10 to 80. The ratio of efflux velocity to wind speed, K, varied from 4 to 16. When K is small entrainment generally increases because the wind is relatively stronger. Several trajectories are plotted for each velocity ratio: K of 2, 5 and 10. These are plotted in dimensionless coordinates of x/D_o and z/D_o where D_o is the source diameter. The highest trajectory (physically the lowest because of negative buoyancy) for each group of common K corresponds to Fr = 5, the lowest to Fr = 50 with Froude number cases 10 and 20 in between. The thin horizontal lines are isopleths of dilution. Dilution of .02 means the original unit mass has increased through entrainment 50 times. The

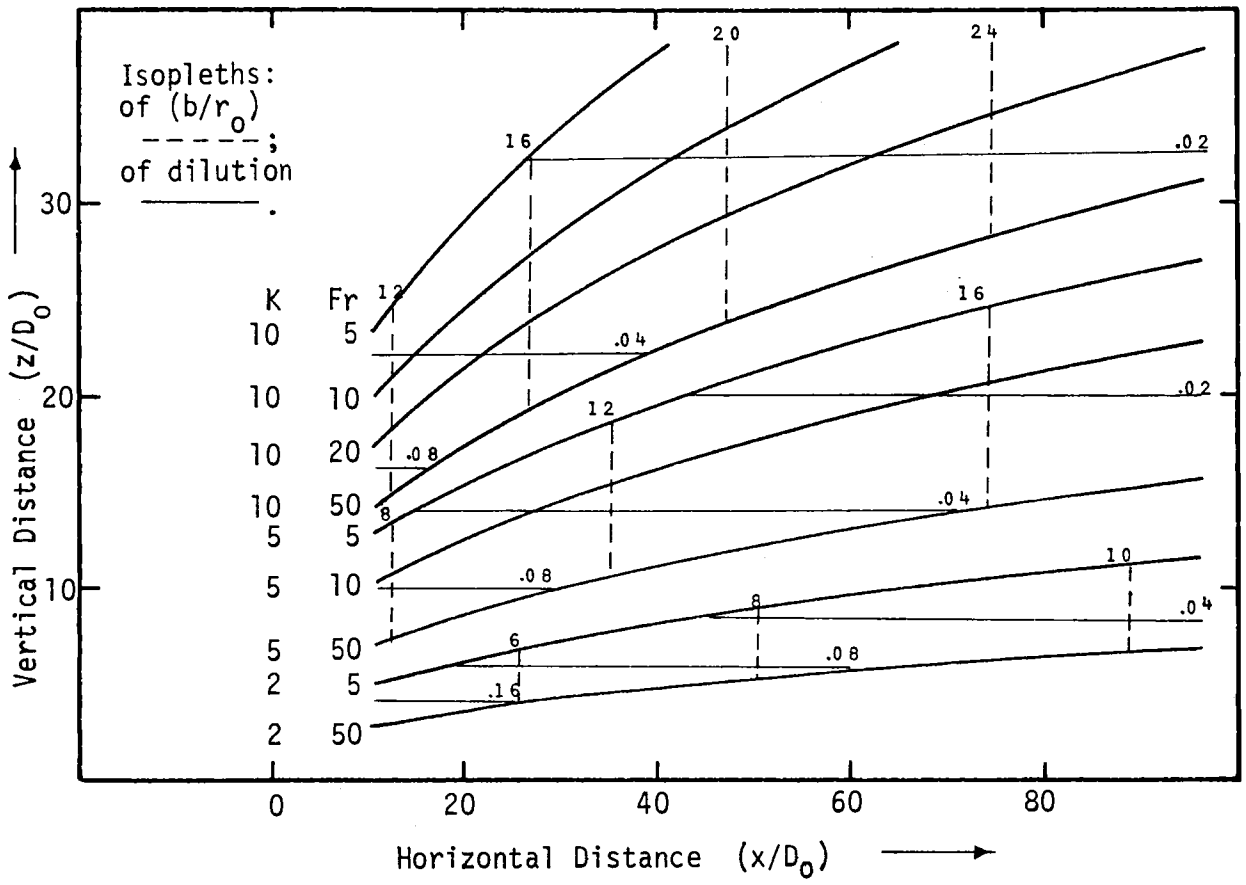

Figure 3. Data Correlation Curves based on Fan's plume data.

thin broken lines are spoken of as isopleths of radii but are actually isopleths of the vertical center half widths. The format is followed in other figures of this kind.

The data correlation curves reproduce the data with about 95% representation so that some distortion can be expected. Even with this considered it is striking that the radius and dilutions isopleths are normal to each other. If the presumption that plume cross sections are round is correct then these isopleths should be approximately parallel to each other. In other words, since these quantities are directly dependent on each other, the larger the observed radius the more diluted the plume must be.

By definition the concentration c is $m_o/(m_o+m_a+m_e)$ where m_o is the mass of tracer (which could be all the mass) in the initial element, m_a is the remaining mass of the initial element and m_e is the mass of entrained fluid at a later time. But $m_o+m_a+m_e = \rho\pi b^2 h$ and $m_o = \rho_o \pi b_o^2 h_o$ where ρ is the density of the fluid, ρ_o is the partial (in the sense of partial pressures) density of the tracer, b_o and h_o are the initial radius and height of the element respectively and b and h are subsequent dimensions. Then $c = (\rho_o b_o^2 h_o/\rho b^2 h)$. If K = 1 then h_o/h is approximately constant and $c = \text{const.}/b^2$. Thus b or b^2 uniquely defines a concentration independent of what the Froude number may be. When K is different from unity then h is not constant and some independence between concentration and radius will be observed.

The fact is, this type of relationship is not experimentally observed, for a given horizontal distance and velocity ratio where the radius remains about constant for varying Froude numbers, the dilutions vary by

as much as a factor of four. A variation of that magnitude means the cross sectional area varies by a factor of four, implying a factor of two variation in the "radius". Similar comments apply in varying degrees to Figure 4 which presents data correlation curves based on experimental data obtained by Chasse and Winiarski (3). Models based on the round plume hypothesis do not, indeed, can not predict this behavior.

Figure 5 shows the results of applying the Lagrangian Plume Model, to be introduced later, when the round plume hypothesis is used. Here entrainment is assumed to be proportional to the wind speed and to the projected area of the plume element with a constant of proportionality of unity. (Other details will be presented in the next section.) In contrast with the isopleths in Figures 3 and 4 the radius and dilution isopleths are nearly parallel. This is the most important difference between observation and model results. (The only effect keeping them from being exactly parallel is the variable rate of contraction of the element along the trajectory due to the influence of buoyancy. Buoyancy changes the rate of decay of velocity along the axis of the plume, this alters the rate of contraction of an element in this direction in turn altering the observed radius.)

Other discrepancies can be noted though it is not clear whether the model can be modified to account for these without changing the shape of the plume profile. In direct contradiction with observation the radii isopleths, never vertical, become even more horizontal with distance from the origin. Overall entrainment does seem adequate because dilutions agree, in a very general way, with the observed

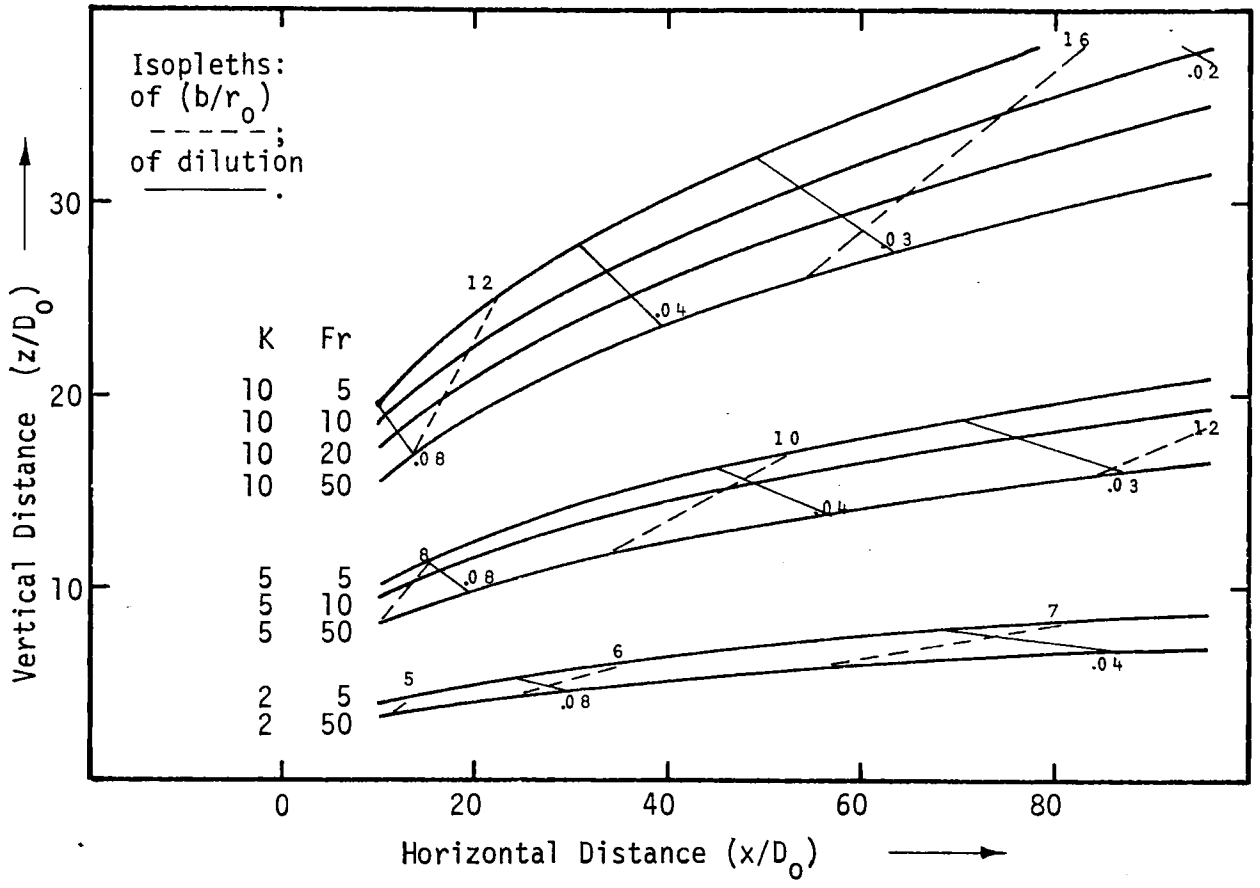

Figure 4. Data Correlation Curves based on EPA plume data (3).

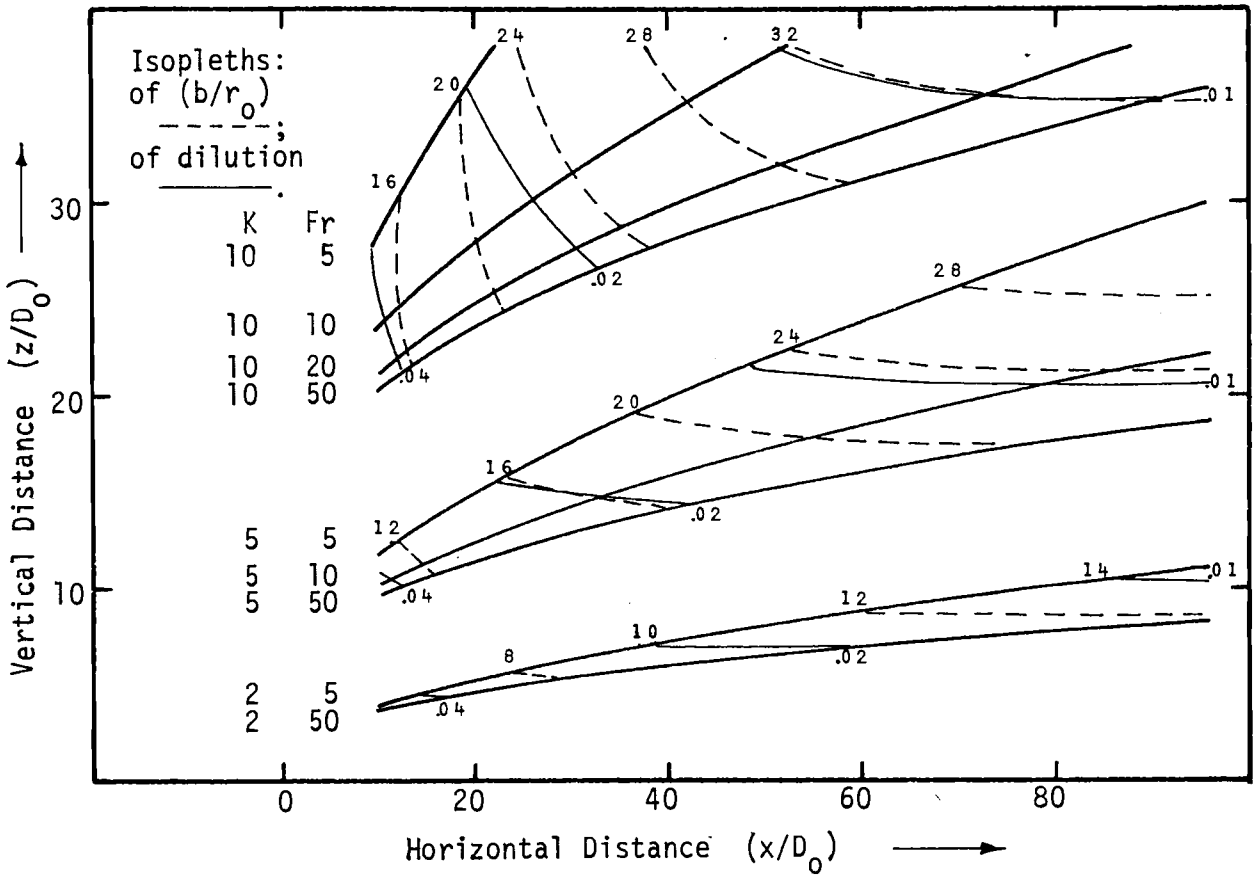

Figure 5. Lagrangian Plume Model results with the round plume assumption.

dilutions[1]. However, trajectories are too high indicating the distribution of entrainment along the trajectory is not expressed correctly (near source differential growth, to be discussed later, is thought to play an important role in describing the behavior more adequately). It should be clear that with all the inherent uncertainty in the data and in the data correlations absolute comparison between numbers is not possible. Still, if the round plume hypothesis were adequate, better agreement with radii would be expected considering that the dilutions are so very similar. Changing the entrainment function can be expected to change some results as desired but, in some cases, correcting one discrepancy will lead to another. Such behavior is expected to require the eventual adoption of a more accurate and detailed cross section.

Having reviewed evidence that suggests plume cross sections are not generally round it is appropriate to search for the mechanisms which cause the differential growth that leads to elliptical cross sections. At least three mechanisms, each indirectly affecting entrainment, are possible. First, pressure gradient forces or differential wind mixing that cause the plume to flatten and bifurcate immediately upon exiting the source. This will be called 'near source differential growth'. Second, differential growth initiated by differential buoyancy inherent in the bending of the plume. This will be called 'curvature induced differential growth'. Finally, differential growth

[1] Fan's dilutions represent centerline maxima while model results are average dilutions. For direct comparison model dilutions should be multiplied by about two. In addition, Fan's trajectories are loci of maxima while the model trajectories relate to the center of mass of the plume.

where the source of differential buoyancy is due to variable amounts of adiabatic cooling or warming due to different amounts of rise in different regions of the plume. This will be called 'adiabatic differential growth'.

III THE LAGRANGIAN PLUME MODEL

One way of illustrating the effects of various mechanisms on plume behavior and structure is to use them in a plume model. The LAGRANGIAN PLUME MODEL, a computer model designed for air and water plumes injected to a cross flow and based on the model developed by Winiarski and Frick (6), was chosen because of its relative simplicity and directness. In this model a parcel of plume mass is defined as it issues from the orifice. The parcel, illustrated in Figure 6, is followed through space as the independent variable, time, increases. From the initial instant the element grows steadily as it mixes environmental fluid with itself. The plume is idealized as a bent cone without the convoluted instantaneous surface of a real plume. Steady state is assumed and entrainment is assumed proportional to the wind speed and to the projected area of the plume parcel.

The projected area is the parcel area exposed to the ambient upstream fluid and projected onto a plane normal to the wind. Looking downwind it would appear as in Figure 6b. Since the projected area of elliptical cross sections will be used later the projected area of that case is studied. The round plume cross section will then be a special case of that relationship. The projected area is found by subtracting the common area of the small ellipse from the farther larger one taking account of the area of the small ellipse outside the projected plane of the larger one. The following expression results:

$$3. \qquad A_{proj} = 2fh\sin\Theta + \pi/2[b\Delta f + f\Delta b][h/(v_c\Delta t)]\cos\theta.$$

Here, as illustrated in Figure 6, v_c is the average total plume parcel

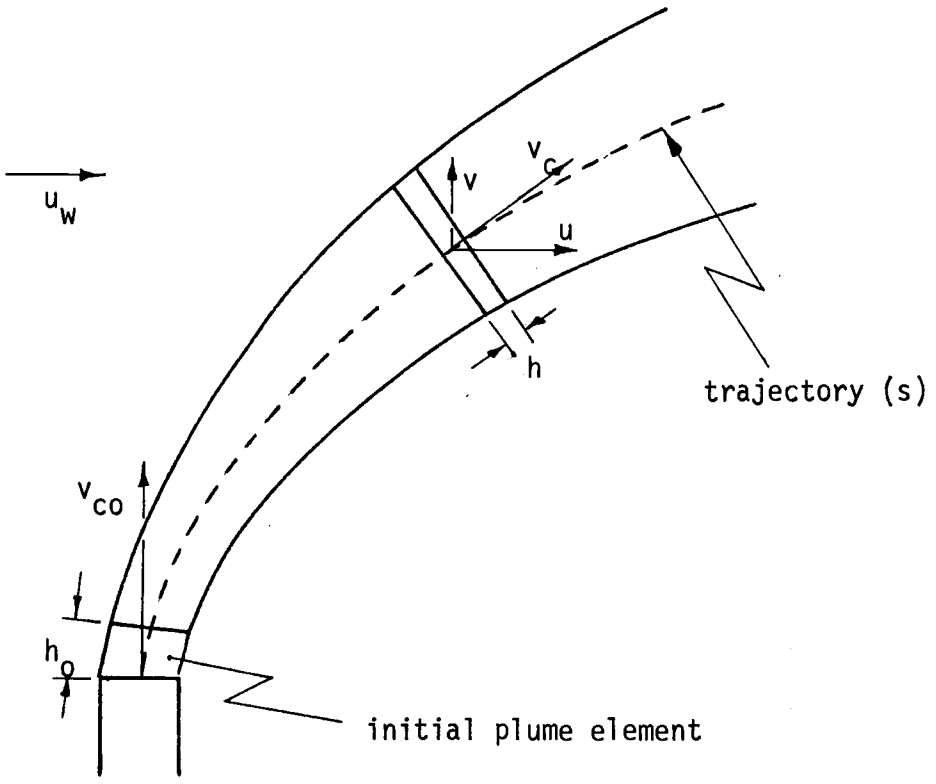

Figure 6a. Plume element at time zero and time t.

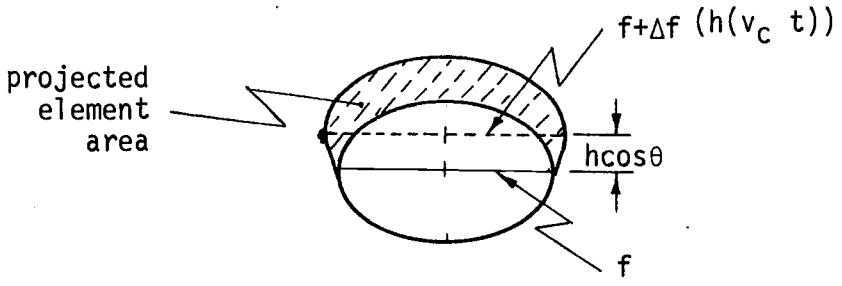

Figure 6b. The projected area of the plume element.

speed, f and b are the half-axes of the ellipse nearest the orifice, Δf and Δb are the increases of the half-axes in time Δt and, when multiplied by the factor $h/(v_c \Delta t)$ are the differences in b and f over the parcel length h. The $\sin\theta$ and $\cos\theta$ factors express the fact that the projected area is dependent on the angle of the centerline to the x-axis. Other variables explained later are also illustrated in Figure 6.

The first term in Equation 3 is the projected area of the upstream portion of the band around a cylinder. The second term is the contribution to the projected area from the growth of the plume over the distance h. This contribution is attributed to the fact that the plume is approximated better by a cone than by a cylinder. This contribution is often neglected but, although initially small relative to the first term, it can be shown that it becomes about equal to it as the plume centerline angle θ becomes small. Another contribution resulting from the curvature of the plume will be neglected. For the round plume, Equation 3 reduces to,

$$4. \qquad A_{proj} = 2fh\sin\theta + \pi b \Delta b[h/(v_c \Delta t)]\cos\theta.$$

The total entrainment into the plume in time Δt is given by,

$$5. \qquad \Delta m = E \rho_a u_w \Delta t A_{proj},$$

where ρ_a is the ambient fluid density, u_w is the wind speed and E is the fraction of impinging fluid effectively captured by the parcel's projected area. In this work the entrainment fraction E is assumed to be unity. Entrainment is assumed proportional to the wind speed u_w because the plume, being in steady state, moves at all points stationary with respect to the orifice, with the relative speed $-u_w$. As a con-

sequence mass flows across the plume-ambient interface with the speed u_w. If this premise is accepted then it can also be shown that entrainment into an individual parcel is also proportional to u_w.

The parcel moves in reaction to forces acting on it and consistent (horizontally) with momentum conservation of the combined parcel and entrained mass. Buoyancy is a force which may be present. Some forces will be neglected; large scale pressure gradient forces will be assumed negligible compared with other forces. Drag is assumed to be zero. This is the result of the one way nature of entrainment: injection of plume fluid into the environment results in growth of the plume just as environmental fluid entering the plume results in growth. This is the case since the environment is defined as the region in which the concentration of plume properties is zero. This means there is not any detrainment and therefore there is not a boundary layer effect due to a plume 'surface'. Thus, conventional drag is absent. (Further details are available in Appendix A.)

Overall combined horizontal momentum conservation means that,

6. $$d/dt(mu) = u_w(dm/dt),$$

where m is the plume parcel mass equal to $\pi\rho fbh$ and u is the horizontal average speed of the parcel within the plume. (See Appendix A for the derivation of Eqns. 6 and 11.) Carrying out the differentiation,

7. $$u\ dm/dt + m\ du/dt = u_w\ dm/dt.$$

Dividing by m and integrating over the time interval t to t+Δt yields,

8. $$u_{t+\Delta t} - u_t = \int_t^{t+\Delta t} du = \int_t^{t+\Delta t} [(u_w - u)(dm/dt)/m]\ dt$$
$$= (u_w - u_t)(\Delta m/m).$$

Rearranging terms,

9. $$u_{t+\Delta t} = u_t + (u_w - u_t)(\Delta m/m).$$

In these equations Δm is the mass entrained by the parcel in time Δt.

If a net buoyancy force is not acting on the plume a similar relationship exists for vertical momentum. Since ambient vertical motion is usually zero a term corresponding to the right hand term of Eq. 6 is zero. For this case,

10. $$v_{t+\Delta t} = v_t - v_t(\Delta m/m)$$

If the plume is buoyant the buoyant acceleration term must be included in which case the vertical equation of motion becomes,

11. $$v_{t+\Delta t} = v_t - v_t(\Delta m/m) + [(\rho_a - \rho)/\rho]\, g\Delta t,$$

where velocities and densities refer to average quantities and g is the acceleration of gravity. There is not general agreement on whether this buoyant term is correctly stated. Some researchers think that this buoyant force affects a greater mass than the mass in which the force finds its origin. These people may speak of virtual masses and, if their point of view is accepted the last term in Eq. 11 might be reduced, commonly by a factor of two (5,8).

When changes in phase do not occur the energy equation is expressed as,

12. $$d/dt(mT) = T_a\, dm/dt - m\Gamma\, dz/dt.$$

Here T is the average parcel temperature and T_a is the temperature of the local environment, and Γ is the adiabatic lapse rate equal to $0.0098^{o}K/m$. The second term on the right is the adiabatic cooling occuring within the plume. Differentiating,

13. $$T\, dm/dt + m\, dT/dt = T_a\, dm/dt - m\Gamma\, dz/dt.$$

If adiabatic cooling is unimportant then, as with Eq. 9,

14. $T_{t+\ t} = T_t + (T_a - T_t)(\Delta m/m)$.

If changes of phase occur this relationship is altered through latent heat release; these complications are dealt with in Appendix B.

Density is computed from the equation of state where temperature is corrected to account for the presence of water vapor.

15. $\rho_{t+\Delta t} = p/[(R_d T_{t+\Delta t})(1 + 0.61 w_{t+\Delta t})]$,

where R_d is the gas constant for dry air and w is the plume water vapor mixing ratio. As long as the plume does not reach saturation the combined water vapor of the parcel and the entrained fluid is conserved. The conservation of total mixing ratio is,

16. $w_{t+\Delta t} = w_t + (w_a - w_t)(\Delta m/m)$,

where w and w_a refer to the mixing ratios of the plume and the environment respectively.

In computing the trajectory $\Delta z = v\ \Delta t$ and $\Delta x = u\ \Delta t$ are added to z and x respectively. The total distance traversed by the parcel in time Δt is,

17. $\Delta s = (\Delta z^2 + \Delta x^2)^{1/2}$.

Due to velocity convergence along the trajectory, s, shrinking or stretching in the parcel length h will occur. Thus,

18. $h_{t+\Delta t} = h_t + [(v_{c(t+\Delta t)} - v_{ct})(h_t/\Delta s)]\Delta t$,

where $v_c = (u^2 + v^2)^{1/2}$. To satisfy continuity a corresponding change in the radius of the element must occur. This is important because entrainment that depends on the parcel's radius will be affected. Since $m = \pi b^2 h \rho$ the resulting radius becomes,

19. $b_{t+\Delta t} = [m_{t+\Delta t}/(\rho_{t+\Delta t} h_{t+\Delta t})]^{1/2}$,

where $m_{t+\Delta t} = m + \Delta m$.

This completes a brief review of the basic Lagrangian Plume Model equations. Water plumes are commonly studied because of their simplicity and because they are amenable to laboratory experiment. A notable difference between the air and water models is the equation of state. The density for water in kg/m^3 is given by:

$$\rho = 1000.0 - 0.00525(T - T_b)^2. \quad (20)$$

This equation is valid in the range 10 - 50°C. Both models are presented in Appendix C.

It is worth noting that the dry model gives results almost identical to those resulting from numerically solving Weil's (14) dry plume equations. In fact, the Lagrangian Plume Model led to the discovery of disparities in Weil's published results. The published comment on Weil's paper is presented in Appendix D. Findings presented in the comment were recently confirmed by Wigley (15). Weil derives his equations from the conventional dynamical and thermodynamical equations in an appendix. Equations 6, 11 and 14 can be derived directly from these.

IV PLUME STRUCTURE APPROXIMATIONS

The easiest way to modify the Lagrangian Plume Model for differential growth resulting in assumed elliptical cross sections would be to simply make the plume dimensions proportional to some plume variable. This would perhaps demonstrate the influence of such cross sections on plume behavior. However it is likely that this method would be subject to some of the same difficulties the round plume hypothesis suffers. It will be much better if some success can be achieved in actually isolating the processes that cause differential growth and describing them quantitatively. This is the purpose of this and the next section.

To determine the effect of differential plume density on buoyancy forces within the plume consider a simple two layer element suspended in a fluid as in Figure 7. This element will experience an overall buoyant acceleration proportional to $g(\rho_a - \rho)/\rho$ where ρ_a is the density of the ambient fluid at pressure p_m, $\rho = (\rho_1 + \rho_2)/2$ is the average element

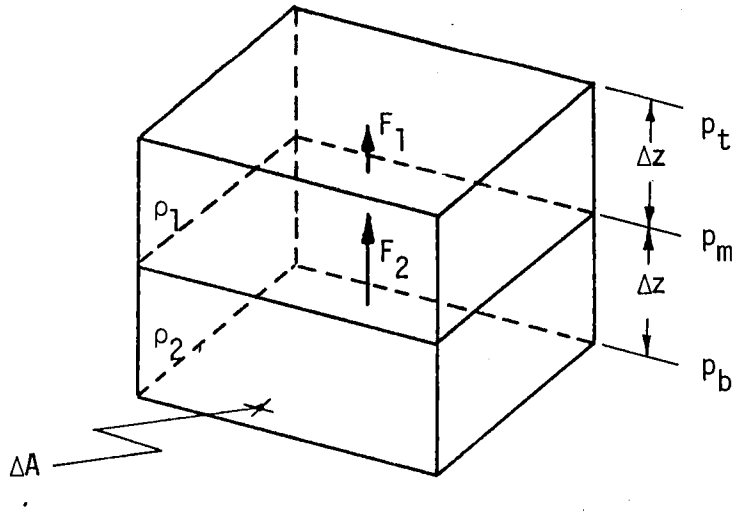

Figure 7. Forces acting on an element composed of two layers of different densities.

density and ρ_1 and ρ_2 are layer average densities. Moreover, due to the different buoyant forces acting on the element's layers there will be an acceleration relative to the element center. In other words, for the case illustrated in Figure 7, the centers of mass of the element's layers will accelerate toward each other.

To understand the nature of this relative acceleration consider the forces acting on the layers. The net force on the upper layer is F_1:

21. $$F_1 = (p_m - p_t)\Delta A - \rho_1 g \Delta V.$$

Similarily the total force on the lower layer is F_2:

22. $$F_2 = (p_b - p_m)\Delta A - \rho_2 g \Delta V.$$

In these equations p refers to the hydrostatic pressure at different heights and the subscripts t, m and b refer to the top, middle and bottom of the element. ΔA and ΔV are the horizontal areas and volumes of the layers. Since $\Delta V = \Delta z \Delta A$, the acceleration a_1 experienced by the upper layer is:

23. $$a_1 = F_1/(\rho_1 \Delta V) = (p_m - p_t)/(\rho_1 \Delta z) - g;$$

and the acceleration of the lower layer a_2 is:

24. $$a_2 = F_2/(\rho_2 \Delta V) = (p_b - p_m)/(\rho_2 \Delta z) - g.$$

The difference between the accelerations, Δa, provides the acceleration of the layers relative to each other:

25. $$\Delta a = a_1 - a_2 = (p_m - p_t)/(\rho_1 \Delta z) - (p_b - p_m)/(\rho_2 \Delta z).$$

Δa is not an incremental quantity because Δz, ΔA and ΔV may be comparatively large. From the hydrostatic equation $\partial p/\partial z = -\rho_a g$ and therefore

26. $$p_m - p_t = -\partial p/\partial z \, \Delta z = \rho_{a1} g \Delta z,$$

and similarly,

27. $$p_b - p_m = -\partial p/\partial z \, \Delta z = \rho_{a2} g \Delta z.$$

Here ρ_{a1} and ρ_{a2} are the average ambient densities outside layer 1 and 2 respectively. Substituting Equations 26 and 27 into Equation 25 yields,

28. $\Delta a = (\rho_{a1} g)/\rho_1 - (\rho_{a2} g)/\rho_2$.

For the case of water plumes or for air plumes where Δz is small enough so that density changes in the environment are small compared with density changes due to temperature changes is the plume,

29. $\Delta a \simeq \rho_a g(\rho_2 - \rho_1)/(\rho_1 \rho_2)$.

To simplify this further it is assumed that deviations in density from the ambient density are small, then,

30. $\Delta a \simeq g(\rho_2 - \rho_1)/\rho_2$:

With further approximations and using the equation of state,

31. $\Delta a \simeq g(T_1 - T_2)/T_1$.

This relative acceleration leads to vertically convergent velocities within the element relative to the translating element center. This tends to increase the density at the center of the element. In turn a pressure gradient field is established that drives a horizontal element expansion. A vertical pressure gradient field is also established that partially counters the relative acceleration, Δa. The latter reflects the fact that the buoyancy forces must do work to produce the kinetic energy now associated with the horizontal divergent velocities (this problem is addressed in the next section).

A more complete idea of what is occuring is now possible. As the element rises or sinks due to its average buoyancy and momentum the element's shape simultaneously deforms because of the relative accelerations and resulting relative velocities. In no way is the trajectory

of the element directly affected. However the surface to volume ratio of the plume will be altered. This will modify the entrainment rate which will in turn cause other plume properties to change.

Figure 8 shows schematically the origin of differential buoyancy in a plume. The diagram shows a plume injected to a cross flow. If the amount of dilution increases with distance from the orifice it follows that the top of the vertical cross section, being farther from the orifice than the bottom, will, under ordinary circumstances, be closer to ambient temperature and density than the bottom. For the case of the warm plume this means the bottom of the cross section is less dense than the top. The resultant Δa leads to vertically convergent

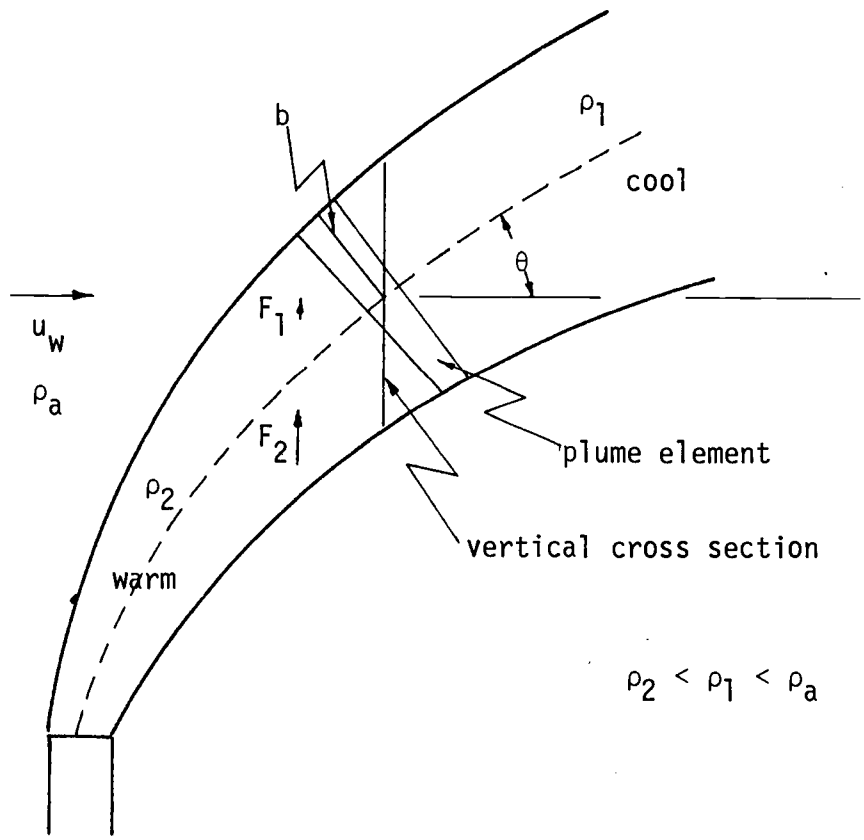

Figure 8. Origin of differential vertical buoyancy in a buoyant plume.

velocities about the center of the element (other effects being ignored for the time being). When the magnitude of the relative velocity generated by Δa is multiplied by the cosine of the plume angle θ the amount of velocity convergence normal to the centerline is obtained. This is differential growth. Due to other mechanisms the plume will usually grow in all directions but the rates of growth will depend on orientation.

A perspective view of a buoyant plume subject to differential growth is presented in Figure 9. The initial round plume element grows

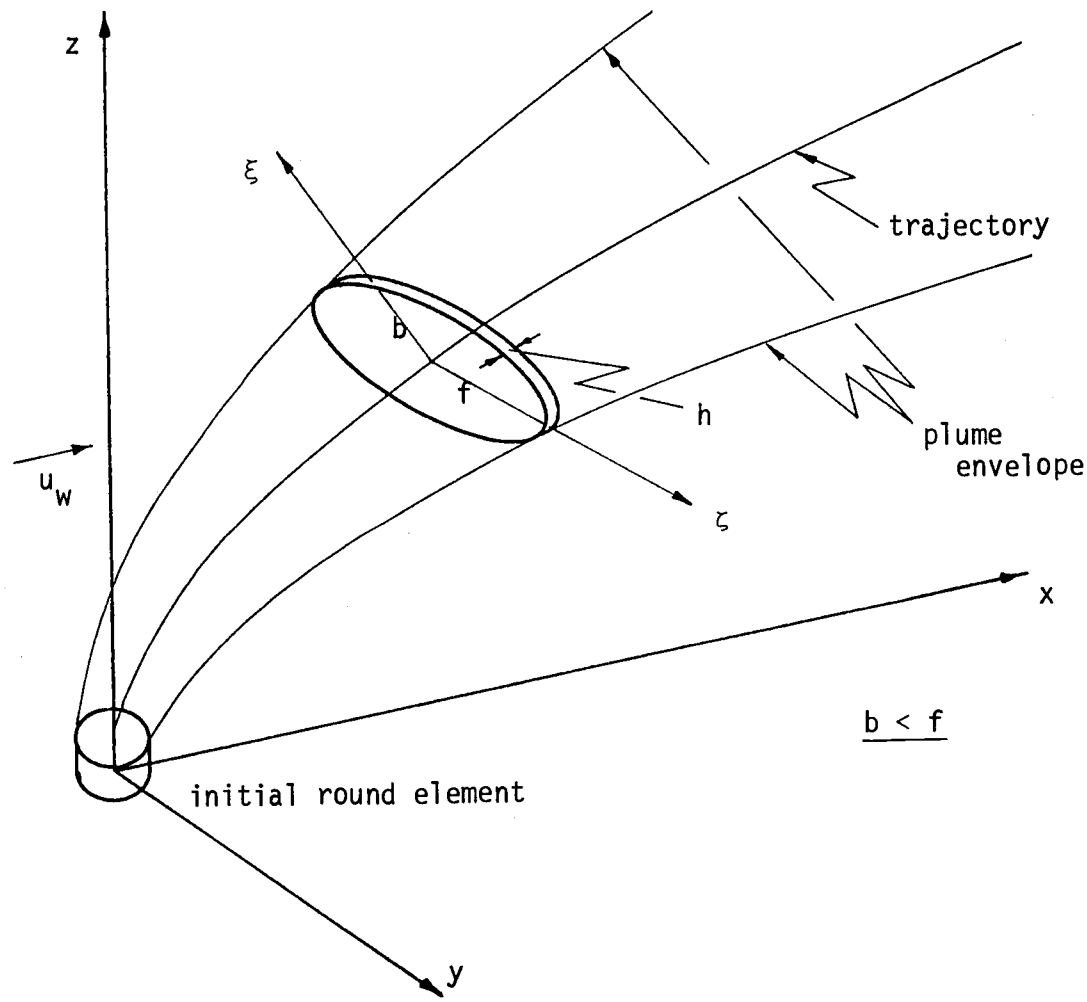

Figure 9. The effect of differential growth on plume structure.

from entrainment and because of different relative velocities deforms into an elliptical cross section. The deformation is two-dimensional and occurs along the ζ and ξ axes. The ζ axis is parallel to the y-axis and has its origin at the center of the element. The ξ axis is normal to the ζ axis and to the centerline; it also has its origin at the center of the element. The plume dimension f is measured along the ζ axis, the dimension b is measured along the ξ axis. Even though the relative acceleration about the element center along the ξ axis is usually small compared to the net buoyant acceleration of the element it can still generate significant relative velocities in time and lead to quite different minor and major axes. Again, the resulting elliptical cross section is still an approximation to reality but will hopefully lead to more realistic model results.

In atmospheric plumes an additional contribution to differential buoyancy must be considered. Plumes rising in air will cool differentially depending on the height reached by a particular region of the plume. In other words, the potential temperature will tend to be constant, horizontally speaking, if the element is well mixed. Under these circumstances the difference in temperature between the top and bottom of the element due to adiabatic cooling is,

$$32. \qquad T_t - T_b = -\Gamma\Delta z,$$

where the subscripts t and b refer to regions near the top and bottom of the element and $\Delta z = 2b\cos\theta$ is the vertical extent of the element. In the surrounding ambient air the corresponding temperature difference is,

$$33. \qquad T_{at} - T_{ab} = dT_a/dz\ \Delta z.$$

The buoyant acceleration near the top of the element is a_t:

34. $$a_t = (T_{at} - T_t)g/T_{at};$$

and near the bottom it is a_b:

35. $$a_b = (T_{ab} - T_b)g/T_{ab}.$$

The relative acceleration $\Delta a = a_t - a_b$ is,

36. $$\Delta a = (T_{at} - T_t)(g/T_{at}) - (T_{ab} - T_b)(g/T_{ab}).$$

Substituting Equation 33 into Equation 36 yields,

37. $$\Delta a = \frac{T_t \, dT_a/dz \, \Delta z + T_{at}T_b - T_tT_{at}}{T_{at}^2 - T_{at} \, dT_a/dz \, \Delta z} \, g.$$

Under most circumstances $T_{at} \, dT_a/dz \, \Delta z$ is much less that T_{at}^2 and T_t/T_{at} is approximately unity. With these approximations Δa becomes,

38. $$\Delta a = (dT_a/dz \, \Delta z + \Gamma \Delta z)g/T_{at}.$$

As implied previously, when the atmosphere is neutrally stratified then $dT_a/dz = -\Gamma$ and the relative acceleration vanishes. This adiabatic differential growth may seem insignificant upon casual inspection but it is thought responsible for the flattening of a plume rising in very stable air.

Several complications not considered in the above simplified model are now briefly addressed. If condensation or evaporation occurs within the plume the adiabatic lapse rate must be replaced by some other lapse rate for which the pseudoadiabatic lapse rate serves as a first approximation. Entrainment in the immediate vicinity of the plumes source requires additional comments also. The necessary near source differential growth is expressed in terms of a velocity difference, Δu,

39. $$\Delta u = [(v_c b)/(2u_w)]\partial u/\partial s \, \Delta s.$$

This expression involves many approximations and is physically very

tentative. However when used in the model this expression allows some insight into the effects of near source differential growth. Details of the derivation of Δu are provided in Appendix D.

V ADAPTING THE LAGRANGIAN PLUME MODEL TO INCLUDE DIFFERENTIAL GROWTH

In Section IV it was indicated that convergent motion along the ξ-axis is necessarily accompanied by compensating divergent motion along the ζ-axis if divergence in h is not permitted. (It can be shown that h is function of v_c only: $h = (v_c/v_{co})h_o$, where v_{co} is the efflux velocity.) It should then be clear that the force leading to Δa, the component parallel to the ξ axis to be referred to as a_ξ, acts not solely to change v_ξ but v_{tot} where $v_{tot} = (v_\xi^2 + v_\zeta^2)^{1/2}$. As explained on page 25 the expressions for a_ξ take account of buoyancy force but not of forces of constraint. In order to find the relationship between $a_\xi \Delta t$ and Δv_ξ the relationship between v_ξ and v_ζ must first be developed. This relationship is found by differentiating the equation for the area of an ellipse, $A = \pi bf$ when A is held constant. Then,

40. $$db/dt = -(b/f)(df/dt),$$

and it is stressed again that this does not refer to changes in b or f resulting from entrainment or convergence of the centerline velocity v_c. Since $v_\xi = db/dt$ and $v_\zeta = df/dt$,

41. $$v_\xi = -(b/f)\, v_\zeta,$$

which means that a change in dimension in the ξ-axis is accompanied by $-b/f$ times that amount of change in the ζ-axis over time Δt.

To find the relationship governing production of the relative velocity v_ξ by the acceleration a_ξ it is necessary to consider how the constraint of two-dimensional mass continuity affects this relationship. The forces causing divergence along the ζ-axis are not known explicity but the energy contained in the horizontal motion can be traced to a_ξ. The change in kinetic energy of relative motion of the plume element

is,

42. $1/2\ d/dt(mv_{tot}^2) = mv_{tot}a_\xi\cos\psi$

where ψ is the angle between the vertical vector $\vec{a}_\xi$ and $\vec{v}_{tot}$. Differentiating and dividing by mv_{tot},

43. $d/dt(v_{tot}) = a_\xi\cos\psi - 1/2(v_{tot}/m)\ dm/dt.$

But,

44. $dv_{tot} = d[(v_\xi^2 + v_\zeta^2)^{1/2}]$
$= (v_\xi dv_\xi + v_\zeta dv_\zeta)/[(v_\xi^2 + v_\zeta^2)^{1/2}].$

Substituting from Equations 40 and 41 ,

45. $dv_{tot} = [1 + (f/b)^2]^{1/2}\ dv_\xi.$

Combining Equations 43 and 45 and changing to finite increment form,

46. $\Delta v_\xi = -(\Delta m/2m)v_\xi + a_\xi\cos\psi[1 + (f/b)^2]^{-1/2}\ \Delta t.$

The angle ψ as well as a_ξ will vary over the cross section in a complicated way. It is assumed that an average value of $\psi = 45^o$ adequately represent this fact. Then,

47. $\Delta v_\xi \simeq -(\Delta m/2m)v_\xi + (0.354a_\xi)[1 + (f/b)^2]^{-1/2}\ \Delta t.$

Remember that the other component of force, ma sin , is opposed by the induced pressure gradient force and does not change the kinetic energy.

This completes the examination of the ramifications stemming from mass continuity. Admittedly many assumptions have been made; it is felt this is necessary to contain the scope of this paper.

It remains then to enumerate expressions for the relative acceleration a_ξ. When $x<r_o$ the bottom of a vertical cross section is at the mouth of the source which complicates a simple expression a_ξ. Because other complications also appear in this region no attempt is made to express a_ξ here. This will introduce some error noticeable especially for low

K cases. When $x > r_o$ it becomes meaningful to represent the vertical density difference, $\rho_{top} - \rho_{bottom}$, in terms of the plume density gradient along the axis of the plume:

48. $$\rho_{top} - \rho_{bottom} = 2b \sec\theta \sin\theta \partial\rho/\partial s,$$

where ρ_{top} and ρ_{bottom} refer to the vertical cross section indicated in Figure 8. The expression for a_ξ becomes,

49. $$a_\xi = [2gb \sin\theta \ \partial\rho/\partial s]/\rho.$$

Instead of using densities, virtual temperatures could be used in a similar expression.

To find the growth of the element due to entrainment the change in area of the element is divided by the circumference of the ellipse. This means that growth due to entrainment is assumed to occur uniformly over the circumference of the ellipse. This change in the dimension b is referred to as Δb_{subt} and equals,

50. $$\Delta b_{subt} = [A_{t+\Delta t} - A_t]/[2\pi\{2/(b^2 + f^2)\}^{1/2}],$$

where A refers to the area of the cross section and t again refers to time. The areas $A_{t+\Delta t}$ and A_t are found from the relationship,

51. $$A = m/(\rho h);$$

the circumference of the ellipse is approximated by $2\pi\{(b^2 + f^2)/2\}^{1/2}$. ($\Delta b_{subt}$ will also include changes resulting from the dependence of A upon $\partial v_c/\partial s$.) Finally, including the differential velocity contribution tion, the total observed change in the dimension b over the time increment Δt is,

52. $$\Delta b_{total} = \Delta b_{subt} - v_{\xi(t+\Delta t)}\Delta t,$$

where $v_{\xi(t+\Delta t)} = v_{\xi t} + a_\xi \Delta t$ found from combining Equations 47 and 49. With Equation 52 the new dimension $b_{t+\Delta t}$ can be found,

53. $b_{t+\Delta t} = b_t + \Delta b_{total}$.

Equation 53 together with the equation for the element area is then used to find the new dimension $f_{t+\Delta t}$:

54. $f_{t+\Delta t} = A_{t+\Delta t}/(\pi b_{t+\Delta t})$.

The incremental change in f, Δf, required in calculating entrainment is,

55. $\Delta f = f_{t+\Delta t} - f_t$.

If near source differential growth is used in the model then, for Δu as expressed in Appendix D,

56. $\Delta b_{\xi n.s.} = 1.57 v_c[(u_{t+\Delta t} - u_t)/(u_w \Delta s)]\Delta t$.

$\Delta b_{\xi n.s.}$ is then added to Δb_{total}.

The results of incorporating these expressions into the Lagrangian Plume Model are described next.

VI DATA AND MODEL COMPARISONS

The basic plume model, the means of dealing with elliptical cross sections and the mechanisms for differential growth have been described. Now the results of applying differential growth concepts to the Lagrangian Plume Model are presented. Figure 10 compares differential growth model results with data correlation curves for Fan's data (shown again to facilitate comparison). The model results come from using curvature induced differential growth. Again, the three groups of curves in each graph represent K's of 2, 5 and 10 from bottom to top respectively. Froude numbers are as indicated. The isopleths of b/r_o, the broken light lines, are labelled at the top of the respective group. The isopleths of dilution, light solid lines, are labelled at the bottom. Considering the uncertainties in the treatment perfect agreement is not expected however it seems fair to make a general kind of comparison. What really matters at this stage of development is whether the model as modified predicts the proper type of relationship between b/r_o and dilution.

Figure 11 compares model results using the round and elliptical plume assumptions. Recall that with the round plume assumption the isopleths of dilution and of b/r_o should, when graphed, be nearly parallel. Basically this is due to the fact that these quantities are then directly dependent upon each other. Comparing the results, with differential growth this direct dependence is broken. The relationship between b/r_o and dilution qualitatively takes on the character revealed by the data correlations of Fan's and of Chasse and Winiarski's data.

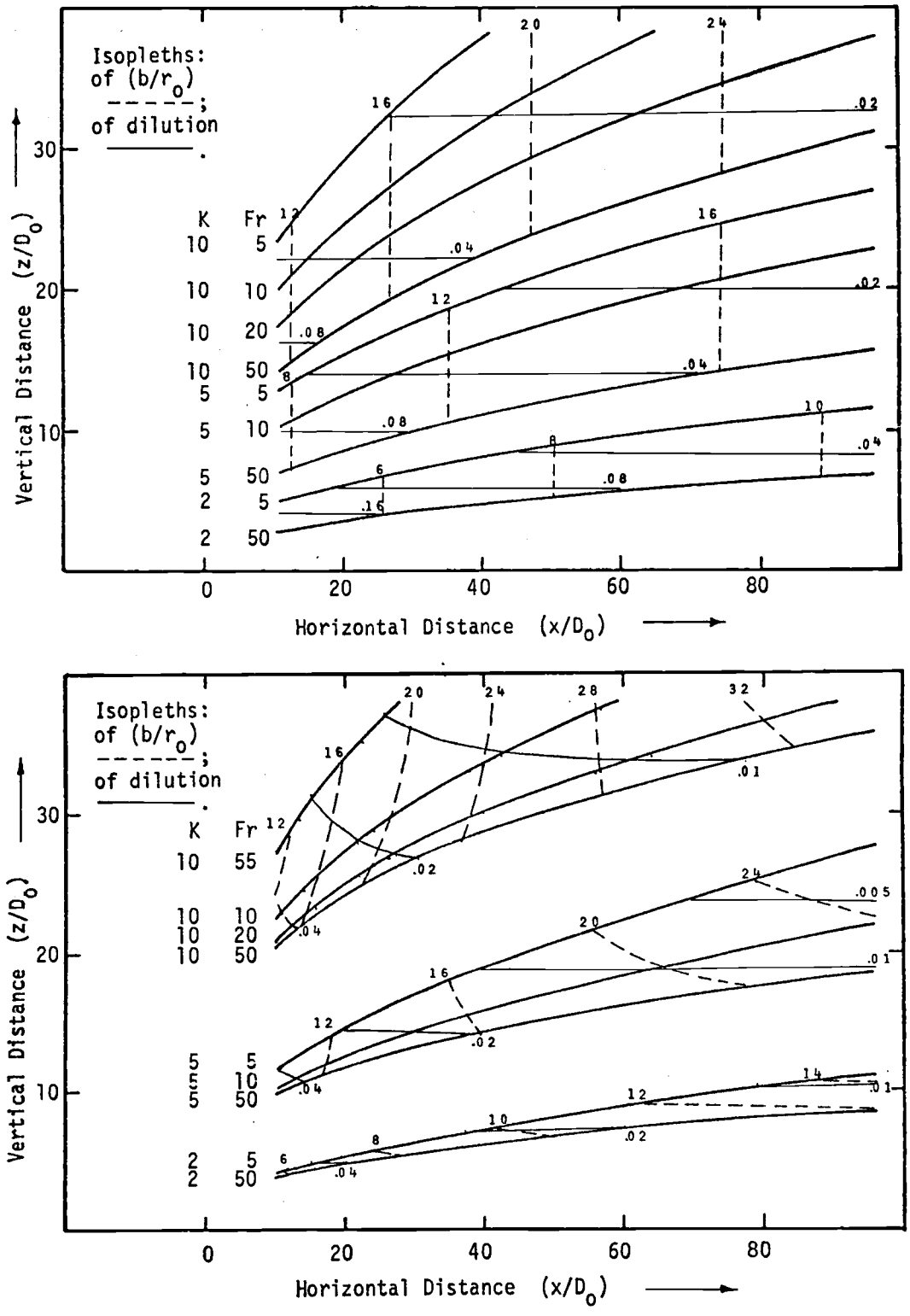

Figure 10. Data correlation curves based on Fan's plume data (top) compared with model results using curvature induced differential growth.

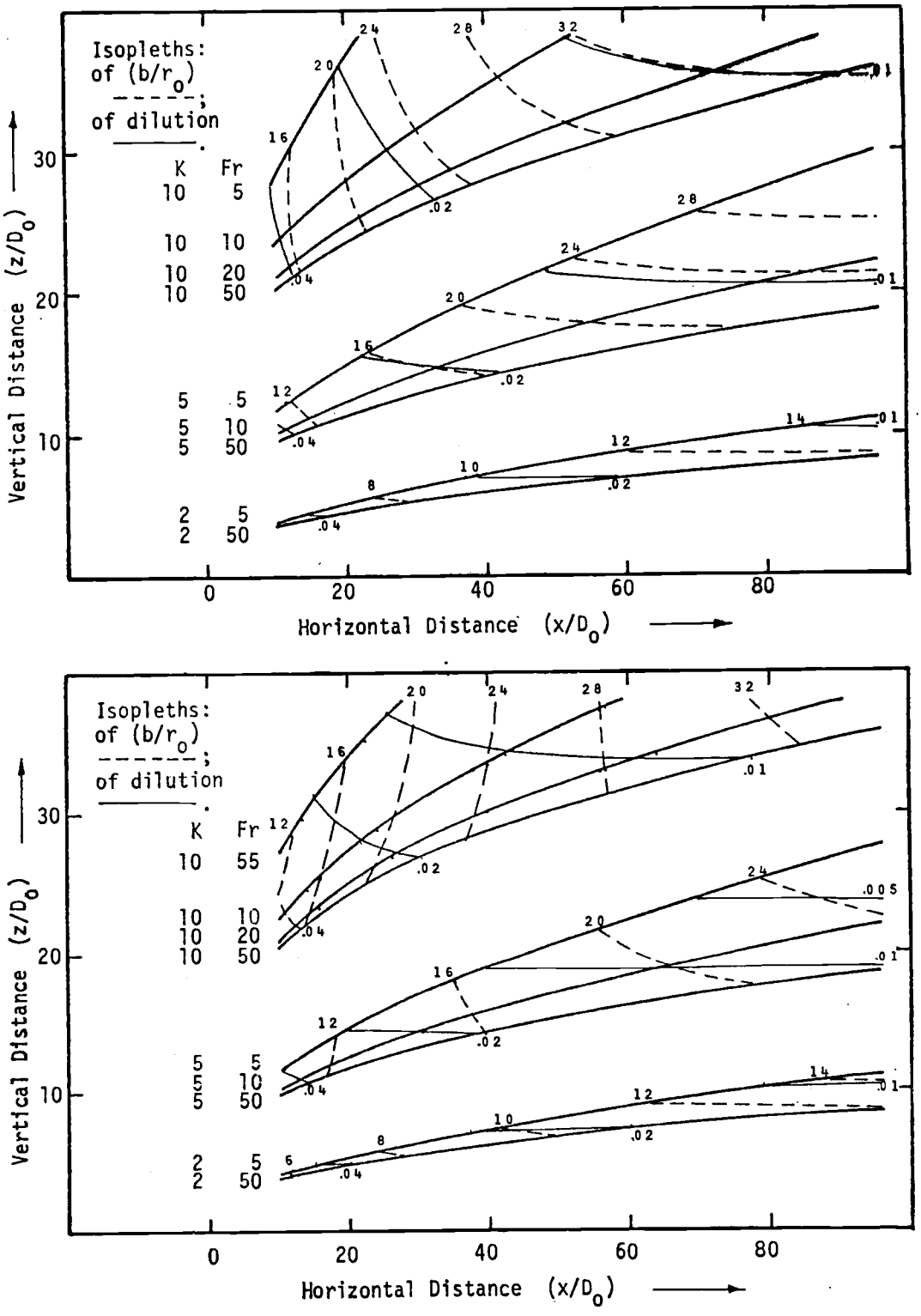

Figure 11. Model results using the round plume assumption (top) vs. differential growth (bottom).

That is to say that the isopleths as displayed are more or less normal to each other. For low values of K this formulation does not result in substantial differences between assumptions probably because the effect is not allowed to begin until $x > r_0$ by which time the element is substantially diluted.

At this point it seems appropriate to analyze other aspects of the comparison between data and model. The trajectories calculated under the current assumption are considerably higher than the correlation curves especially at small values of x/D_0. This becomes more apparent examining the loci of actual experimental trajectories in Figure 12. Note that here the trajectories for small x/D_0 are even lower than the correlation counterpart. The data correlations fail in the region where near source differential growth is thought to play an important part in plume dynamics (this is discussed later). These comments also apply when comparisons with Chasse and Winiarski's data are made. (It should be noted that in correlation curves of their data the dimensions plotted are measured vertically whereas b is calculated normal to the trajectory.) Notice also how the trajectory heights bunch together at small x/D_0 in Figure 12. In this regard the model is generally more realistic than the data correlation curves.

In Figure 13 the effect of differential growth on the plume cross section is illustrated. The elliptical cross section is superimposed on Fan's cross section for Froude number of 20 and k of 8. Aside from the indentation in the bottom, the general shape of the cross section is approximated. The sizes would be more equal had it been possible for Fan to plot the zero concentration isopleth.

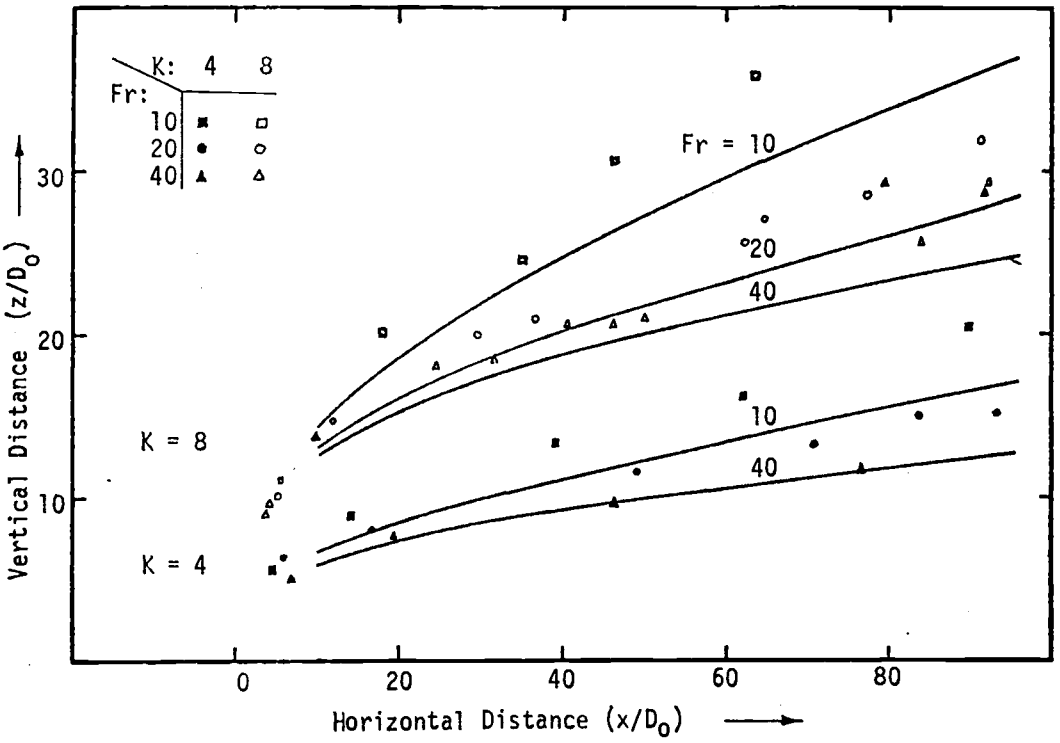

Figure 12. Comparison of model results with near source differential growth (lines) with actual data points obtained by Fan.

So far model findings have used the virtual mass concept. This means that the buoyancy term for the vertical equation of motion was divided by two. Physical justification for its use may be found in references 4 and 7. Its use permits better agreement than is achieved otherwise.

The findings already discussed explain some aspects of plume behavior very well. Trajectories and isopleths of b/r_0 and dilution agree grossly with the data correlation curves. However, as already indicated, the data correlation curves differ somewhat from the raw data points. It has been mentioned that near source differential growth is thought important in explaining the differences between model results and experimental data.

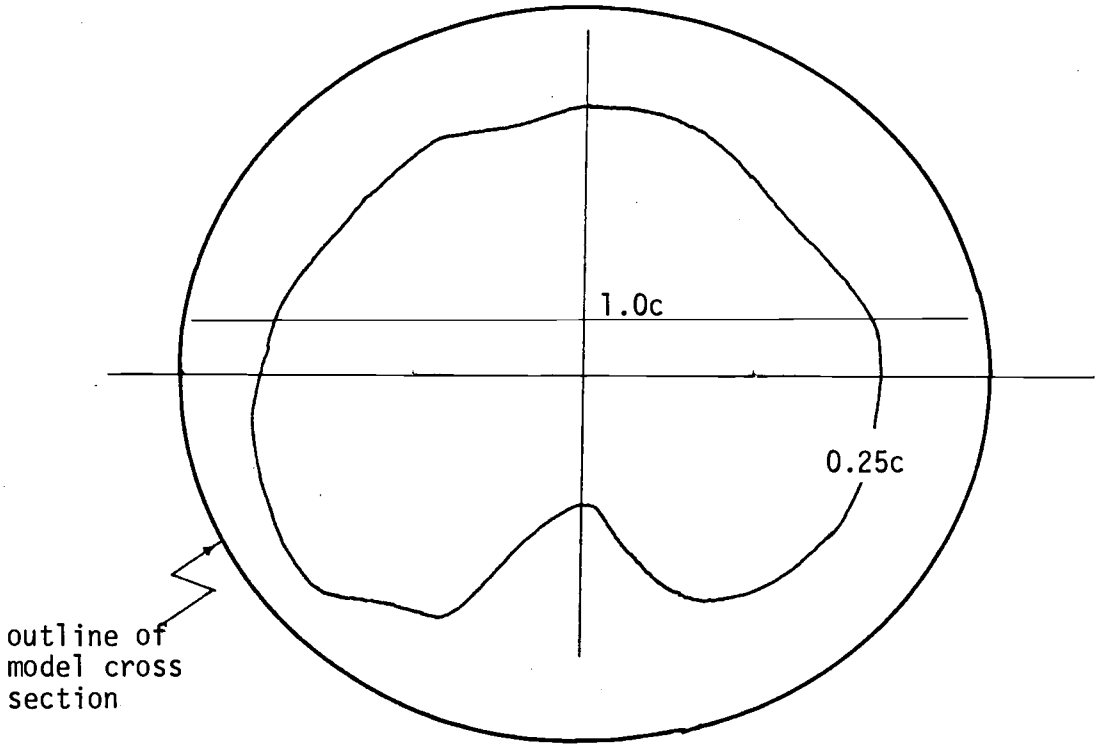

Figure 13. Model cross section compared with Fan's experimentally obtained cross section for Fr. = 20, K = 8, and s/D_o = 37.0.

In order to get some idea as to the effect of near source differential growth Equation 56 can be used in the model; the results are also shown in Figure 12. Curvature induced differential growth was not used in obtaining these results. (This neglect will cause dilution and b/r_o to be interrelated more except for cases with large Froude numbers where there is little differential growth.) The agreement between model results and raw data are good for large Froude numbers, however, for small Froude numbers the formulation of near source differential growth represented by Equation 56 is far too powerful. The plume rise is substantially lowered even though the virtual mass concept has been temporarily put aside to obtain these results. Several reasons for the inadequacy of Equation 56 are suggested in Appendix E.

CONCLUSION

The round plume assumption should be examined. There are several experiments that have looked at plume cross sections and most of those indicate some departure from roundness. Though this is important for its own sake, most important is the effect of the consequent increased projected cross section on enhancing entrainment into the plume. Entrainment is in turn of first order importance in determining the plume's behavior.

After examining experiments and the physical aspects of the problem, three mechanisms leading to the deformation of the cross sections suggest themselves. These were called "curvature induced", "adiabatic" and "near source" differential growth. These were defined in preliminary terms and adapted to the Lagrangian Plume Model. More work needs to be done to define these mechanisms more accurately, however, the modifications made on the basic model only changed the shape of the cross sections and thereby the entrainment. In no way was the basic model altered. The absolute correctness of the differential growth mechanisms is not of primary importance since the purpose of the paper is to demonstrate the effects of the mechanisms.

Aside from the shortcomings above, the basic model generally makes the same assumptions made throughout plume theory. In this way it shares many of the same weaknesses. Foremost of theseis the assumption that the plume boundary merges smoothly with an undisturbed ambient environment. Other criticism may be expressed. Certainly the problem could be approached with the Eulerian Navier-Stokes equations but it has proven difficult to express the eddy stress terms in much simpler

applications.

Hopefully these comments will help keep the problem in perspective. Plumes exist and understanding their behavior is important. The current state of understanding is far from complete. The aspects of plume behavior discussed in this paper will help complete the picture even though more important questions may have to be answered. With that, it is urged that someone demonstrate conclusively that plume cross sections depart significantly from roundness and that this bears on the plume's behavior. Relatively simple photographic or transmissometer work would go far in satisfying this need.

BIBLIOGRAPHY

1. Abramovich, G. The Theory of Turbulent Jets. MIT Press, 1963.

2. Ayoub, G.M. "Test Results on Buoyant Jets Injected Horizontally in a Cross Flowing Stream". Water, Air and Soil Pollution, 2, pp. 409-426, 1973.

3. Chasse, J. and Winiarski, L. Laboratory Experiments of Submerged Discharges with Current. PNERL Working Paper #12, Pacific N.W. Envrn. Rsrch. Lab., Ntnl. Envrn. Rsrch. Cntr., Corvallis, Oregon. ORD USEPA, June 1974.

4. Davies-Jones, R.P. "Discussion of Measurements Inside High-Speed Thunderstorm Updrafts." J. of Applied Meteorology, 6, pp. 710-717, 1974.

5. Fan, L.N. Turbulent Buoyant Jets into Stratified or Flowing Ambient Fluids. Report KH-R-15, W.M. Keck Lab. of Hydraulics and Water Resources, Calif. Inst. of Tech., 1967.

6. Frick, W.E. and Winiarski, L.D. "Comments on 'The Rise of Moist Buoyant Plumes'" J. of Applied Meteorology, 3, p. 421, 1975.

7. Hamilton, P.M. "The Application of a Pulsed-Light Rangefinder (LIDAR) to the Study of Chimney Plumes", Philo. Trans. of the Roy. Soc. of London, A 265, pp. 153-172, 1969.

8. Hewett, T.A., Fay, J.A., Hoult, D.P. "Laboratory Experiments of Smokestack Plumes in Stable Atmosphere", Atmospheric Environment, Pergamon Press, Vol. 5, pp. 767-789, 1971.

9. Hirst, E.A. Analysis of Round, Turbulent Jets Discharged to Flowing Stratified Ambients, Oak Ridge National Lab., Report ORNL_4685, June 1971.

10. Lamb, Sir Horace, Hydronamics Dover Publication, N.Y. pp. 684-686.

11. Overcamp, T.J. and Hoult, D.P. "Precipitation in the Wake of Cooling Towers." Atmospheric Environment, Vol. 5 pp. 751-765, 1971.

12. Scorer, R.S. Natural Aerodynamics Pergamon Press, New York, 1958.

13. Shirazi, M.A., Davis L.R., and Byram, K.V. Effects of Ambient Turbulence on Buoyant Jets Discharged into a Flowing Environment. PNERL Working Paper #2, Pacific N.W. Envrn. Rsrch. Lab., Ntnl. Envrn. Rsrch. Cntr., Corvallis, Oregon. ORD USEPA, January 1973.

14. Weil, J. "The Rise of Moist Buoyant Plumes", J. of Applied

Meteorology, 4, pp. 435-443, 1974.

15. Wigley, T.M.L. "A Numerical Analysis of the Effect of Condensation on Plume Rise", J. of Applied Meteorology, 6, pp. 1105-1109, 1975.

16. Winiarski, L. and Frick, W. Cooling Tower Plume Model, Thermal Pollution Branch, PNWRL, NERC EPA, Corvallis, Oregon. 1975.

17. Vehrencamp, J.E., Ambrosio, A. and Romie, F.E. "Convection from Heated Sources in an Inversion Layer", First Report of Air Pollution Studies, Report 55-27, UCLA Dept. fo Engineering, 1955.

APPENDICES

APPENDIX A

A simple proof of Equations 6 and 11 is developed below. This proof makes use of several assumptions commonly found in plume theory. First, the Boussinesq approximation is made in evaluating the buoyancy force. Second, the pressure in the plume is assumed to be the hydrostatic value of the horizontally adjacent ambient pressure. Third, all plume boundary variables go to the local ambient value. Fourth, stresses, conduction and diffusion are neglected along plume element boundaries inside the plume. Fifth, as a simplifying assumption the wind is assumed constant with height and the plume is assumed small relative to length scales of significant ambient change.

With these assumptions in mind, suppose the frame of reference is fixed in the ambient fluid, itself in uniform motion everywhere with respect to the source. In this coordinate system the momentum of the plume element can be described by $m(\vec{v}_{av}-\vec{u}_w)$. Here m is defined by $\int_V \hat{\rho} dV$, $\vec{v}_{av}$ is the average velocity of the element as measured in the source frame and defined by $1/m\int_V \vec{v}\hat{\rho}dV$ where V is the volume of the element at a given instant. Finally, $-\vec{u}_w$ is the velocity of the plume source relative to the ambient coordinate system. At the moment of discharge the relative momentum is $m_o\vec{v}_{avo}-m_o\vec{u}_w$. By virtue of assumptions three and four the only significant force that can act on the element is the buoyancy force, if present. This follows from Newton's Second Law: the forces must be zero at the elements outside boundaries. If there is not a buoyancy force then it follows that the momentum of the element is constant. But generally,

57. $$d/dt(m(\vec{v}_{av}-\vec{u}_w)) = m\vec{g}(\rho - \rho_a)/\rho.$$

Here ρ is defined by $1/V\int_V \hat{\rho} dV$. For the horizontal equation of motion

58. $d/dt(m(u - u_w)) = 0.$

Recalling that u_w is constant and rearranging terms,

59. $d/dt(mu) = mg(dm_a/dt).$

This is Equation 6. The vertical component is equivalent to Equation 11:

60. $d/dt(mv) = mg(\rho_a - \rho)/\rho.$

In deriving an expression for the buoyancy force recall that the buoyant force per unit volume is given by $g(\rho_a - \rho)$. The total force on the element is then,

61. $$g\int_V(\rho_a - \hat{\rho})dV = g\int_V \rho_a dV - g\int_V \hat{\rho} dV$$
$$= g\rho_a dV - gV((1/V)\int_V \hat{\rho} dV).$$

But the average element density ρ of the plume element is defined by $(1/V)\int_V \hat{\rho} dV$ and by definition $V = m/\rho$. Thereby the buoyancy force is as expressed in Equation 60.

APPENDIX B

Saturation and condensation are encountered when the mixing ratio of the mixed element (i.e. m + Δm) is greater than the saturation mixing ratio for the mixed element at the mixed temperature. Figure 6 describes moist thermodynamic processes.

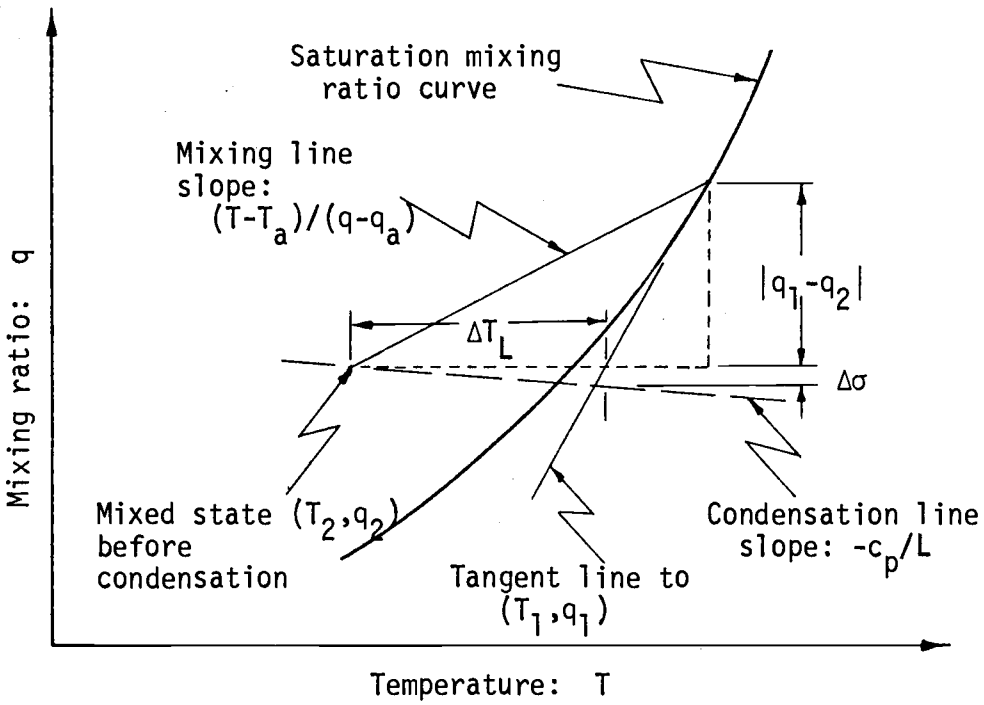

Figure 14. Moisture thermodynamics.

Suppose the element is initially in state (T_1,q_1), as it mixes with ambient fluid condensation proceeds continuously but it is equivalent to suppose that the element mixes in small steps. First it mixes without condensation and reaches state (T_2,q_2) after a mass, Δm, mixes into the element. At this point temperature T_2 is substituted into the integrated Clausius-Clapeyron equation; this results in the saturated mixing ratio for T_2, that is q_{2s}:

62. $$q_{2s} = k_1 \exp[(L/R_v)(T_{t+\Delta t} - T_f)/(T_f T_{t+\Delta t})].$$

Here L and R_v are the latent heat of condensation and the gas constant of water vapor respectively. T_f is a reference temperature (273 K) and $k_1 = 0.0038$ is the constant of proportionality corresponding to T_f. Comparing mixing ratio results in $q_2 > q_{2s}$ which is the criterion for condensation. In the next step condensation occurs along the path of condensation until the temperature is reached where there is not any supersaturated vapor. The slope of the path of condensation is $-c_p/L$ and is nearly horizontal so that the temperature rise ΔT_L caused by condensation can be approximated by,

63. $$\Delta T_L = (T_1 - T_2) - [R_v/(L/T_1^2)][q_1 - q_2].$$

The second term on the right is the slope tangent to the saturation curve at (T_1, q_1) multiplied by $(q_1 - q_2)$. This quantitiy ΔT_L multiplied by $-c_p/L$ gives the amount of liquid water mixing ratio condensed out. The change in liquid water mixing ratio, $\Delta\sigma$, is,

64. $$\Delta\sigma = \sigma_2 - \sigma_1 = (c_p/L)\Delta T_L.$$

The adjusted amount of liquid water mixing ratio in the element becomes,

65. $$\sigma_{t+\Delta t} = \sigma_t + (\sigma_a - \sigma_t)(\Delta m/m) + \Delta\sigma,$$

where σ_a and σ refer to the liquid water mixing ratio content of the environment and the element respectively.

At this point the vapor mixing ratio must be corrected; simply subtracting $\Delta\sigma$ will lead to iteration errors because the new estimate will not fall exactly on the saturation curve. After many iterations this can lead to serious errors. Instead the adjusted temperature $T_2 + \Delta T_L$ is used in the integrated Clausius-Clapeyron equation to find the new mixing ratio. Note that this will overestimate the amount of

vapor condensed.

Evaporation begins when (T_2, q_2) falls below the saturation curve. This is handled the same way: the signs simply reverse. The entire treatment of moisture variables is similar to the method described by Overcamp and Hoult (11) and attributed to Bezold and Brunt.

In this model precipitation is assumed not to form because generally the plume element is saturated for only a short time. Due to this assumption the liquid water mixing ratio, σ, contributes to the net density of the element. The density expression must also account for the change in density caused by the presence of water vapor. Using the equation of state $\rho_{t+\Delta t}$ is:

66. $$\rho_{t+\Delta t} = \frac{0.622\ p_{t+\Delta t}}{(0.622 + q_{t+\Delta t})\ R_d T_{t+\Delta t}} (1 + q_{t+\Delta t} + \sigma_{t+\Delta t}),$$

where R_d is the gas constant for dry air, $p_{t+\Delta t} = p_t + \partial p/\partial z\ \Delta z$ is the atmospheric pressure, and $T_{t+\Delta t} = T_t + \Delta T_L$.

APPENDIX C

Computer listing of the Lagrangian Plume Model for water.

```
      PROGRAM H2ODIFFX
      DATA (R=287.),(G=9.8),(TWO=2.),(PI=3.1416) ,(P622=.622),(EL=2500.)
     1,(RV=.461),(T273=273.),(ES0=6.11),(ZERO=0.),(CPD=1.003) ,(DD=1.)
     2,(HHOC=.00525),(ONETHOU=1000.),  (BASET=1.5),(ONE= 1.),(P0=1.5708)
     3,(POT= 6.2832)
13    FORMAT(1X,3F7.3,F7.5,4E10.2,F7.2,3F8.4,F7.2,3E8.1)
11    FORMAT (12E9.2,4E6.2)
6     FORMAT (9F8.5,I8)
      DO 999 K= 1,12
      READ(60,6)V,UW,T,TA,H,E,A,B,DT,LUL
      E= B
      IF (EOF(60)) CALL EXIT
      Z= X= TIME=DZ=DB=BSAVE=ZWEI=DH=S =U=ST=VS=DE=DVS=PP=RATIOZ=ZERO
      RATIOX=ZERO
      BA= B
      BO= B*TWO
      VEL= SQRT(U*U+ V*V)
      DENA=ONETHOU-HHOC*(TA-BASET)*(TA-BASET)
      DEN= ONETHOU-HHOC*(T-BASET)*(T-BASET)
      DEN1= DEN
      PM= PM0= PI*B*B*H*DEN
      IF ( UW .NE. ZERO) AK= VEL/UW
      FR= VEL/SQRT((DENA-DEN)/DEN*TWO*B*G)
      DT= 1.4/SQRT(VEL*VEL*AK*AK/20. +UW*UW)/1300*AK/10.  /2.
      DTT= DT/30.
      WRITE (61,7)
7     FORMAT(" ***************************************************************"/
     1"0     TEMP AM TEMP  HOR VEL  VER VEL      WIND       DIA     THICK*TI
     2ME STEP                                    K  FROUDE                  ")
      WRITE(61,11 )T,TA,U,V,UW,BO,H,DT,ZERO,ZERO,ZERO,AK,FR
      WRITE (61,8)
8     FORMAT(" -----SUBSEQUENT PLUME VALUES-----"/"      X/D     Z/D     B/
     1D   THICK      MASS  DEL MASS      ZWEI     DEL B   TEMP  HOR-VEL  VE
     2R-VEL TOT-VEL    S/D                          ")
      LUL= 2000
      DBI= ZERO
      UOLD= U
      AREA0= PM/DEN/H
      DO 99  J= 1, LUL
      EINS=    DENA*UW*DT*TWO*F*H*V/VEL
      ZWEI=    DENA*UW*DT*PO     *(B*DE+F*DB)*H/DD*U/VEL
      DM= EINS+ ZWEI
      SUM= PM+DM
      U= (PM*U+DM*UW)/SUM
      T= (PM*T+ DM*TA)/SUM
      DEN= ONETHOU-HHOC*(T-BASET)*(T-BASET)
      BUO= (DENA-DEN)*G/DEN*DT/TWO
      V= PM*V/SUM+ BUO
      V1= VEL
      PM= SUM
      VEL= SQRT(U*U+ V*V)
```

```
      DZ= V*DT
      DX= U*DT
      DD= VEL*DT
                                          IF(X .LT. BA)GO TO 65
      DVS=(DEN-DEN1)/DEN/DD*G*DT*B*V/VEL/SQRT(ONE+F*F/B/B)-DM/PM*VS/TWO
      VS=VS+ DVS
   65 DEN1= DEN
      FSAVE= F
      DH= (VEL-V1)/DD*H*DT
      H= H+ DH
      AREA= PM/DEN/H
      DB= (AREA-AREA0)/PDT   *SQRT(TWO/(B*B+F*F))
      AREA0= AREA
      DBI= (U-UOLD)/DD*DT*B/UW*VEL*.157/(ONE+BUO*SUM/DM/V)
      UOLD= U
      DB= DB-DBI- VS*DT
      B= B+DB
      F= AREA/PI/B
      DF=(F- FSAVE)
      X= X+ DX
      Z= Z+DZ
      DT= DT+DTT
      IF(J/200-(J-1)/200 .NE. 1) GO TO 99
      RATIOX= X/BO
      RATIOZ= Z/BO
      RATIOR= B/BA
      RATIOF= F/BA
      WRITE(61,13) RATIOX,RATIOZ,RATIOR,H,PM,FINS,ZWEI,DB,T,U,V,VEL
     1,RATIOF, VS,DVS,PP
      IF (RATIOX .GT. 100. .OR. RATIOZ .GT. 40.) GO TO 999
   99 CONTINUE
  999 CONTINUE
      CALL EXIT
      END
```

÷1.41

Computer listing of the Lagrangian Plume Model for air.

```
      PROGRAM DIFAIR
      DIMENSION TT(10), QSS(10)
      DATA (R=287.),(G=9.8),(TWO=2.),(PI=3.1416) ,(P622=.622),(EL=2500.)
     1,(RV=.461),(T273=273.),(ESO=6.11),(ZERO=0.),(CPD=1.003)
     2,(ADIA=.0098),(ONE=1.), (SIXI=.61)
11    FORMAT (2F7.1,3F7.2,2E10.2,4F7.4,2F7.2,2F8.4,2F7.3)
13    FORMAT(1X,3F7.3,F7.5,4E10.2,F7.2,3F8.4,F7.2,F6.4,2E9.2)
      DO 999 KAY= 1,5
6     FORMAT (9F8.5,I8)
      READ(60,6) V,UW,T,TA,H,A,E,B,DT,LUL
      IF (EOF(60)) CALL EXIT
      READ (60,6) U,DTO,Q,QA, SIG ,SIGA ,P,DUW
      AK= SQRT(V*V+U*U)/UW
      DEN =P/R/T /(ONE+SIXI*Q )*(ONE+SIG)
      DENA=P/R/TA/(ONE+SIXI*QA)*(ONE+SIGA)
      FR= V/SQRT((DENA-DEN)/DEN*TWO*B*G)
      DT= ONE/SQRT(VEL*VEL*AK*AK/29.+UW*UW) *AK/5.
      DTT= DT/100.*3.
      Z= X= DZ=S=DH                                    =ZERO
      BA= B
      BO= B*TWO
      WRITE (61,7)
7     FORMAT(" ***********************************************************"/
     1"0       T      TA       U       V      UW       B          H          DT
     2   SIG    SIGA      QA       Q       K      FR      DTO      DUW       A
     3   E")
      WRITE(61,11 )T,TA,U,V,UW,B ,H,DT,SIG,SIGA,QA,Q,AK,FR,DTO,DUW,A,E
      WRITE (61,8)
8     FORMAT(" -----SUBSEQUENT PLUME VALUES-----"/"      X/D     Z/D     B/
     1D   THICK       MASS  DEL MASS       ZWEI      DEL B   TEMP HOR-VEL VER
     2R-VEL TOT-VEL    S/D  MIX R. LIQ HHO      ")
      VEL= SQRT(U*U+ V*V)
      PM= PI*B*B*H*DEN
      DO 99 J= 1,LUL
      DELT=0.
      TA=. TA- DTO*DZ
      DP= -DENA*G*DZ
      P= P+DP
      EINS= E*DENA*UW*DT*TWO*B*H*V/VEL*V/ABS(V)
      IF (DB .LT. ZERO) DB= ZERO
      ZWEI= E*DENA*UW*DT*PI/TWO*(B*DF+E*DB)*H/DD*U/VEL
      DM= EINS+ ZWEI
      AREAD= PM/DEN/H
      SUM= PM+DM
      U= (PM*U+DM*UW)/SUM
      QSS    =  ESO  *EXP(EL/RV*((T-T273)/T273/T))/1000. *P622
      TS= T
      T= (PM*T+ DM*TA)/SUM      -ADIA*DZ
      QS1    =  ESO  *EXP(EL/RV*((T-T273)/T273/T))/1000. *P622
      Q= (Q*PM+QA*DM)/SUM
      IF (Q .GT. QS1 .OR.  SIG .GT. ZERO) GO TO 110
      GO TO 111
110   DTEM= ((T-TA)/(Q-QA)-P622*RV*(T+TS)*(T+TS)/4./QS1/EL/(QSS+P622))*(
     1QSS-Q)
      DSIG= DTEM*CPD/EL
      T= T+ DTEM
      SIG= (SIG*PM +SIGA*DM)/SUM + DSIG
```

```
      IF (SIG. LT. ZERO) SIG= ZERO
      Q     =  ESO  *EXP(EL/RV*((T-T273)/T273/T))/1000. *P622
  111 CONTINUE
      DEN =P/R/T /(ONE+SIXI*Q )*(ONE+SIG)
      DENA=P/R/TA/(ONE+SIXI*QA)*(ONE+SIGA)
      V= (PM*V      )/SUM          +(DENA-DEN)*G/DEN*DT
      PM= SUM
      V1= VEL
      VEL= SQRT(U*U+ V*V)
      DZ= V*DT
      DX= U*DT
      DD= SQRT(DZ*DZ+ DX*DX)
      DVS=-(-.0098-DTO)*B*G/T*U/VEL*TWO
      IF (X .LT. BA) DVS= ZERO
      VS= PM*VS/SUM*B/F+ DVS
      FSAVE= F
      BSAVE= B
      AREA= PM/DEN/(H+DH)
      DB= (AREA-AREA0)/TWO/PI*SQRT(TWO/(B*B+F*F))
      B= B+DB
      DB= DB        -VS*DT
      B= B-VS*DT
      F= AREA/PI/B
      DF=(F- FSAVE)
      DH= (VEL-V1)/DD*H*DT
      H= H+DH
      DT= DT+ DTT
      X= X+ DX
      Z= Z+DZ
      S= S+ DD
      IF (J .LE. 2) GO TO 98
      IF(J/100-(J-1)/100 .NE. 1) GO TO 99
   98 RATIOZ= Z/B0
      RATIOF= F/BA
      RATIOS= S/B0
      RATIOR= B/BA
      RATIOX= X/B0
      WRITE(61,13) RATIOX,RATIOZ,RATIOR,H,PM,EINS,ZWEI,DB,T,U,V,VEL
     1,RATIOF, VS,DVS
   99 CONTINUE
  999 CONTINUE
      CALL EXIT
```

APPENDIX D

Comments on "The Rise of Moist, Buoyant Plumes"

WALTER FRICK AND LARRY WINIARSKI

Thermal Pollution Branch, Environmental Protection Agency, Corvallis, Ore. 97330

27 December 1974

While this article was interesting and informative, Fig. 3 is misleading. A numerical solution of Weil's equations for the 30 m tower radius listed results in a dry plume trajectory about 20% lower than indicated in Fig. 3. A comparison is shown in the figure below. As a check on the numerical solution for Weil's equation, also shown is an independent solution obtained from a simple Lagrangian finite-difference model we have developed. In order to make the comparison meaningful, we have used the same entrainment assumption that Weil used. This solution compares closely with the direct integration of Weil's equation.

We surmised that Weil's trajectory resulted from solving his equation for a point source rather than the finite tower radius listed. Subsequent private communication with Weil has confirmed that the results shown in his Fig. 3 were for a case of zero initial radius and zero initial momentum flux, but with a finite buoyancy flux calculated from the cooling tower conditions listed.

We feel that the differences resulting from these simplified assumptions can be significant.

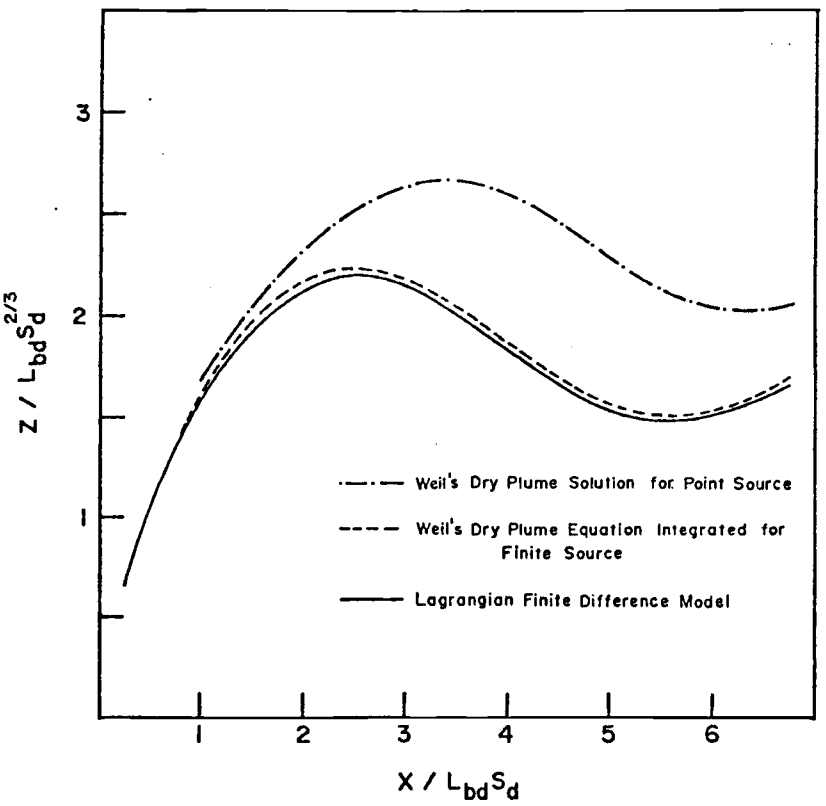

APPENDIX E

Near source differential growth can be approximated if the velocity convergence across the cross section is known. A way of describing the velocity convergence across the section is to presume a time lag, τ, between the horizontal components of velocity on opposite sides of the plume. In other words, at a given level near the source the amount of entrainment is not uniformly distributed; therefore there will exist velocity convergence across the plume element. τ is assumed proportional to the average distance across the plume and inversely proportional to the wind, u_w:

67. $$\tau = (\pi b/2)/u_w,$$

where $\pi b/2$ is the average distance across a circular cross section. The velocity difference across a plume element Δu is then,

68. $$\Delta u = k\, \partial u/\partial s \;\; v_c \tau,$$

where k is a constant of proportionality (equal to unity for now). In finite difference form,

69. $$\Delta u = [(u_{t+\Delta t} - u_t)/\Delta s][v_{ct}\pi b/(2u_w)].$$

Finally,

70. $$\Delta b_{\xi n.s.} = 1.57 v_c[(u_{t+\Delta t} - u_t)/(u_w \Delta s)]\Delta t.$$

Abramovich's cross sections become about four times wider than they are deep at 3.8 diameters along the centerline. Fan's cross sections become quite round at about 30 diameters along the centerline so that this differential growth mechanism must decay rapidly. Presently this can not be expressed except by arbitrarily terminating the mechanism at some point. It seems that near source differential growth is closely tied to the vortex forming process. In the buoyant plume the element

is stretched relative to the nonbuoyant case by buoyant increases in the vertical velocity. This increases the vorticity of the vortices and reduces the time lag τ. These complications will not be pursued further now; the coarse relationship for Δu developed above will be used to gain some appreciation for the consequences growing out of near source differential growth.